

**Figure 3.** Effects of ARB on gene expression of proinflammatory factors, and immunohistochemical expression of PDGF and MCP-1. a, Effect of olmesartan on relative mRNA levels of various proinflammatory factors and NADPH oxidases 7 days after stenting in normal controls (□, n=8), the no-treatment group (▨, n=8), and the ARB-treated group (■, n=8). \* $P < 0.01$  vs uninjured normal artery; † $P < 0.05$ , vs the control group. b, Iliac artery sections from the uninjured normal animals and those from the control and olmesartan groups 10 days after stenting stained immunohistochemically with PDGF-BB and MCP-1. \* indicates stent strut. Bar=100  $\mu$ m. These immunohistochemical experiments were repeated 5 times, all with representative results.

ment with olmesartan partly attenuated the increased DHE fluorescence after stent implantation.

#### Inhibitory Effects of ARB on Inflammatory Changes and Apoptotic Cell Death in Rabbits

As we reported previously,<sup>15</sup> inflammatory changes and apoptotic cell death became evident 7 to 10 days after stent implantation in rabbits (Figure 2a and 2b). Treatment with olmesartan reduced such inflammatory changes and enhanced cell death in the intima after stenting.

#### Inhibitory Effects of ARB on Expression of Proinflammatory Factors and NADPH Oxidase Subunits

Treatment with olmesartan reduced the increased mRNA levels of monocyte chemoattractant protein (MCP)-1, interleukin (IL)-1 $\beta$ , tumor necrosis factor- $\alpha$ , p22phox, and gp91phox in rabbits (Figure 3a). Olmesartan did not affect the increased levels of IL-6 and transforming growth factor- $\beta$ . Immunohistochemical staining performed 10 days after stenting revealed increased immunoreactive platelet-derived growth factor (PDGF)- $\beta$  and MCP-1 in cells in the neointima and in smooth muscle cells in the media. This was attenuated by olmesartan treatment (Figure 3b). Treatment with olmesartan did not affect neovascularization in the neointima and adventitia or re-endothelialization 28 days after stenting (data not shown).

#### Effects of ARB on Transdifferentiation of Mononuclear Cells to Vascular Progenitor Cells

To investigate the potential contribution of vascular progenitor cells, peripheral blood mononuclear cells (MNCs) were

isolated and cultured to stimulate the differentiation into SMPCs or endothelial progenitor cells (EPCs), as described previously.<sup>16,17</sup> The cells cultured in the PDGF-BB-enriched and basic fibroblast growth factor-enriched medium exhibited a hill and valley morphology that is characteristic of smooth muscle cells within 2 weeks. The smooth muscle cell phenotype was confirmed by immunostaining with antibodies specific for smooth muscle cell markers: SMPCs expressed  $\alpha$ -smooth muscle actin (SMA), myosin, and calponin, which were all detected in human coronary artery smooth muscle cells and were not detected in MNCs and Cos-7 cells (data not shown). Expression of  $\alpha$ -SMA gene in SMPCs was also confirmed by PCR analysis (data not shown). As reported,<sup>16,17</sup> the expression of inflammatory markers (MCP-1, IL-1 $\beta$ , etc) was greater in SMPCs than in cultured rabbit aortic smooth muscle cells (data not shown). The cells cultured in the vascular endothelial growth factor-enriched medium exhibited the typical cobblestone morphology of EPCs. The EPCs stained positively for von Willebrand factor and VE-cadherin and incorporated acetylated low-density lipoprotein (data not shown).

Analysis of colony-forming areas showed that the degree of transformation to SMPC was greater in MNCs from animals fed a high-cholesterol diet than in those from untreated, normal animals (Figure 4A). The transformation to SMPCs further enhanced in MNCs from animals that underwent stenting. Treatment of rabbits with olmesartan for 5 to 7 days suppressed the increased transformation to SMPCs induced by stenting. In contrast, there were no differences in the degree of transformation to EPCs among the groups. Immunohisto-

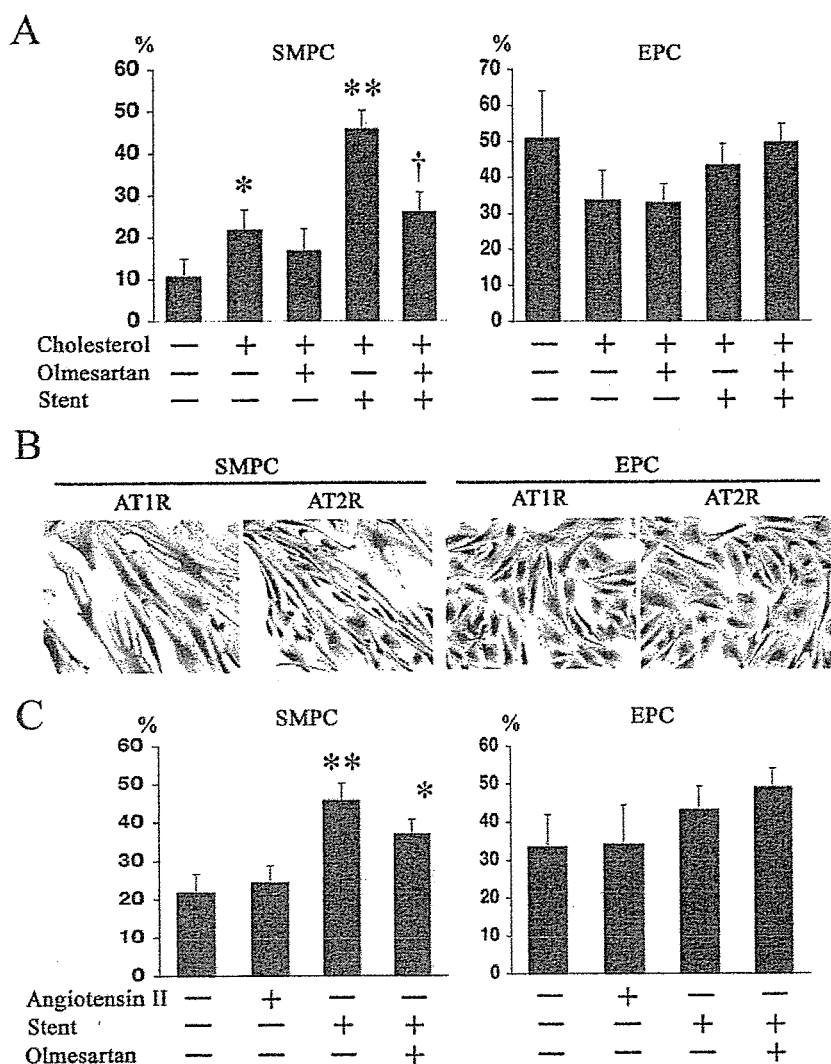


**Figure 4.** Effects of ARB on transdifferentiation of MNCs to SMPCs or EPCs. a, The degrees of transformation of MNCs to SMPCs (the percentages of  $\alpha$ -SMA-positive area per well) or EPCs (the percentages of von Willebrand factor-positive area per well) in normal rabbits and those that received the high-cholesterol diet, high-cholesterol diet plus in vivo olmesartan treatment, high-cholesterol diet and stenting, or high-cholesterol diet, in vivo olmesartan treatment, and stenting (n=8 to 9 each). \* $P$ <0.05, \*\* $P$ <0.01 vs control (cholesterol [-] olmesartan [-] stent [-]). † $P$ <0.05 vs high-cholesterol diet plus stenting (cholesterol [+] olmesartan [-] stent [+]). b, Immunohistochemistry for AT1 receptor and AT2 receptor in SMPCs and EPCs. c, The degree of transformation of MNCs from rabbits fed a high-cholesterol diet to SMPCs or EPCs. The effects of in vitro addition of angiotensin II were examined. In addition, the in vitro effects of olmesartan on the stent-induced increase in transformation were examined (n=8 to 9 each). \* $P$ <0.05, \*\* $P$ <0.01 vs control (angiotensin II [-] olmesartan [-] stent [-]).

chemical staining was then performed to examine the presence of AT<sub>1</sub> receptor and AT<sub>2</sub> receptor. Both receptors were found in SMPCs and EPCs (Figure 4B). We considered the possibility that AT<sub>1</sub> signals might be involved in increasing the transformation capacity of MNCs and, therefore, examined the effects of in vitro administration of angiotensin II or olmesartan on the transformation of MNCs. Angiotensin II did not enhance transdifferentiation, and olmesartan did not suppress transdifferentiation in vitro (Figure 4C).

#### Plasma ARB levels and Arterial Blood Pressure

The maximum drug concentration ( $C_{max}$ ) levels of olmesartan at 15 mg/kg per day and valsartan at 50 mg/kg per day were  $107 \pm 17$  and  $300 \pm 24$  ng/mL, respectively. The  $C_{max}$  level of olmesartan at 3 mg/kg per day was  $537 \pm 24$  ng/mL in rabbits. Therefore, the dose of olmesartan used in rabbits is within a clinically relevant dose range. The  $C_{max}$  levels after oral administration of olmesartan at 5, 10, and 20 mg/body in hypertensive subjects are reported to be  $149 \pm 21$ ,  $273 \pm 17$ , and  $470 \pm 23$  ng/mL (n=6, each), respectively. The  $C_{max}$  values after oral administration of valsartan at 80 and 160 mg/body in hypertensive subjects are reported to be

$2830 \pm 920$  and  $5260 \pm 2300$  ng/mL, respectively, according to the manufacturer's interview form. Thus, the doses of olmesartan and valsartan used in the present study are within or below the clinically relevant dose range.

Treatment with olmesartan showed no effect on systolic and diastolic arterial pressure. Systolic and diastolic pressure were  $94 \pm 2$  and  $59 \pm 5$  mm Hg in the control group and  $92 \pm 2$  and  $52 \pm 6$  mm Hg in the olmesartan group.

#### Discussion

We have demonstrated for the first time that oral treatment with 2 types of ARBs (valsartan and olmesartan) attenuated in-stent neointimal formation in nonhuman primates (cynomolgus monkeys), supporting the conclusions of the VALPREST and VALVACE trials,<sup>12,13</sup> which involved a relatively small number of patients. Although it is uncertain which animal model is most appropriate for the evaluation of in-stent neointima formation (restenotic changes), a nonhuman primate model may have an advantage over nonprimate animal models, because vascular inflammatory and proliferative responses to injury in nonhuman primates are more similar to those in humans than are other, nonprimate models.

Hence, the use of nonhuman primates may work for evaluation of the efficacy of ARB on in-stent neointima formation in clinically relevant conditions.

To obtain mechanistic insight into the beneficial effects of ARB, we first examined the time course of local expression of RAS components in rabbits (Figure 2). We found that expression of all of the components (ACE, angiotensin II, AT<sub>1</sub> receptor, and AT<sub>2</sub> receptor) increased, mainly in cells composed of neointima (monocytes and smooth muscle cells), at early stages (7 to 10 days after stenting), and persisted until 28 days after stenting. This RAS activation colocalized with increased NADPH oxidase-dependent DHE fluorescence (generation of superoxide anion) and was associated with increased levels of NADPH oxidase subunit mRNAs, consistent with previous reports showing that increased reactive oxygen species can be detected in activated smooth muscle cells after balloon injury.<sup>21,22</sup> These *in vivo* observations are also consistent with previously published *in vitro* data suggesting that proliferation and migration of smooth muscle cells are critically mediated by oxidative stress via AT<sub>1</sub>-mediated activation of NADPH oxidases.<sup>23–29</sup> Interestingly, treatment with ARB not only attenuated the levels of oxidative stress markers but also reduced the level of immunoreactive AT<sub>1</sub>. These data suggest the presence of a positive feedback loop in which activation of AT<sub>1</sub> further enhances expression and activity of the AT<sub>1</sub> receptor *in vivo*, as seen in the present study.

It is known that oxidative stress-induced inflammatory and proliferative processes are central to neointima formation after vascular injury.<sup>24,25</sup> We and others have demonstrated that<sup>1</sup> increased monocyte-mediated inflammation or MCP-1 expression is associated with greater neointima formation after stenting,<sup>26,27</sup> and<sup>2</sup> anti-MCP-1 gene therapy<sup>15,28–30</sup> or administration of blocking antibody against the MCP-1 receptor<sup>31</sup> markedly reduces neointima formation after vascular injury. However, no previous study examined whether or not those inflammatory and proliferative changes after stenting depends on the AT<sub>1</sub> receptor. In the present study, we, therefore, examined the effects of ARB on monocyte recruitment and MCP-1 expression after stenting and found that ARB reduced monocyte/macrophage recruitment, as well as MCP-1 immunoreactivity and gene expression. Furthermore, ARB inhibition increased the expression of growth-promoting factors, such as PDGF and IL-1 $\beta$ . These data suggest that the beneficial effects of ARB may be attributed to the inhibition of oxidative stress-induced inflammatory and proliferative changes.

Recent studies have shown that peripheral blood contains bone marrow-derived progenitor cells, which contribute to neointima formation after injury.<sup>16,18,32</sup> However, the role of RAS in the recruitment/differentiation of progenitor cells into the neointimal cells after stenting has not been addressed. Here we found that differentiation to SMPCs increased in MNCs from rabbits fed a high-cholesterol diet and was further enhanced in those rabbits that had also undergone stenting. Differentiation into EPCs was not affected by either the diet or stenting. *In vivo* treatment with ARB suppressed the increased differentiation into SMPCs induced by diet or stenting. In contrast, *in vitro* treatment with angiotensin II or ARB did not affect the capacity to differentiate into SMPCs

or EPCs. Therefore, the capacity to recruit or form SMPCs from MNCs after stenting might be determined by an AT<sub>1</sub> receptor-mediated pathway *in vivo* and, thus, contribute to in-stent neointima formation.

It must be mentioned that ARB did not significantly reduced arterial blood pressure in rabbits. Although arterial pressure was not measured in monkeys, the dose of ARB used in the present study is reported to show no effects on arterial blood pressure in monkeys.<sup>33</sup> Plasma ARB level was within or below the clinical range. Furthermore, ARB did not affect serum lipid levels. Therefore, the beneficial effect of ARB on in-stent neointimal formation is likely to be independent of its effects on arterial blood pressure or serum lipid.

### Perspectives

This study provides experimental evidence suggesting that oral treatment with ARB at a clinical dose range attenuates in-stent neointima formation in rabbits and nonhuman primates. The beneficial effects were associated with reduced local oxidative stress, reduced expression of MCP-1 and other inflammation-promoting factors, and reduced recruitment/differentiation of SMPCs, suggesting that ARB is of potential clinical benefit in patients who have undergone vascular interventions.

### Sources of Funding

This study was supported by Grants-in-Aid for Scientific Research (14657172 and 14207036) from the Ministry of Education, Science, and Culture, Tokyo, Japan; by Health Science Research Grants (Comprehensive Research on Aging and Health, and Research on Translational Research) from the Ministry of Health Labor and Welfare, Tokyo, Japan; and by the Program for Promotion of Fundamental Studies in Health Sciences of the Organization for Pharmaceutical Safety and Research, Tokyo, Japan.

### Disclosures

None.

### References

1. Topol EJ, Serruys PW. Frontiers in interventional cardiology. *Circulation*. 1998;98:1802–1820.
2. Hoffmann R, Mintz GS, Dussaillant GR, Popma JJ, Pichard AD, Satler LF, Kent KM, Griffin J, Leon MB. Patterns and mechanisms of in-stent restenosis. A serial intravascular ultrasound study. *Circulation*. 1996;94:1247–1254.
3. Holmes DR Jr, Leon MB, Moses JW, Popma JJ, Cutlip D, Fitzgerald PJ, Brown C, Fischell T, Wong SC, Midei M, Snead D, Kuntz RE. Analysis of 1-year clinical outcomes in the SIRIUS trial: a randomized trial of a sirolimus-eluting stent versus a standard stent in patients at high risk for coronary restenosis. *Circulation*. 2004;109:634–640.
4. Stone GW, Ellis SG, Cox DA, Hermiller J, O'Shaughnessy C, Mann JT, Turco M, Caputo R, Bergin P, Greenberg J, Popma JJ, Russell ME. One-year clinical results with the slow-release, polymer-based, paclitaxel-eluting TAXUS stent: the TAXUS-IV trial. *Circulation*. 2004;109:1942–1947.
5. Rioufol G, Finet G, Ginon I, Andre-Fouet X, Rossi R, Vialle E, Desjoux E, Convert G, Huret JF, Tabib A. Multiple atherosclerotic plaque rupture in acute coronary syndrome: a three-vessel intravascular ultrasound study. *Circulation*. 2002;106:804–808.
6. Daemen MJ, Lombardi DM, Bosman FT, Schwartz SM. Angiotensin II induces smooth muscle cell proliferation in the normal and injured rat arterial wall. *Circ Res*. 1991;68:450–456.
7. Bell L, Madri JA. Influence of the angiotensin system on endothelial and smooth muscle cell migration. *Am J Pathol*. 1990;137:7–12.
8. Tharaux PL, Chatziantoniou C, Fakhouri F, Dussaulte JC. Angiotensin II activates collagen I gene through a mechanism involving the MAP/ER kinase pathway. *Hypertension*. 2000;36:330–336.

9. Ruiz-Ortega M, Lorenzo O, Suzuki Y, Ruperez M, Egido J. Proinflammatory actions of angiotensins. *Curr Opin Nephrol Hypertens*. 2001;10:321-329.
10. Prasad A, Koh KK, Schenke WH, Mincemoyer R, Csako G, Fleischer TA, Brown M, Selvaggi TA, Quyyumi AA. Role of angiotensin II type 1 receptor in the regulation of cellular adhesion molecules in atherosclerosis. *Am Heart J*. 2001;142:248-253.
11. Wolf G. Free radical production and angiotensin. *Curr Hypertens Rep*. 2000;2:167-173.
12. Peters S, Gotting B, Trummel M, Rust H, Brattstrom A. Valsartan for prevention of restenosis after stenting of type B2/C lesions: the VAL-PREST trial. *J Invasive Cardiol*. 2001;13:93-97.
13. Peters S, Trummel M, Meyners W, Koehler B, Westermann K. Valsartan versus ACE inhibition after bare metal stent implantation—results of the VALVACE trial. *Int J Cardiol*. 2005;98:331-335.
14. Ohishi M, Ueda M, Rakugi H, Okamura A, Naruko T, Becker AE, Hiwada K, Kamitani A, Kamide K, Higaki J, Ogihara T. Upregulation of angiotensin-converting enzyme during the healing process after injury at the site of percutaneous transluminal coronary angioplasty in humans. *Circulation*. 1997;96:3328-3337.
15. Ohtani K, Usui M, Nakano K, Kohjimoto Y, Kitajima S, Hirouchi Y, Li XH, Kitamoto S, Takeshita A, Egashira K. Antimonocyte chemoattractant protein-1 gene therapy reduces experimental in-stent restenosis in hypercholesterolemic rabbits and monkeys. *Gene Ther*. 2004;11:1273-1282.
16. Sata M, Saiura A, Kunisato A, Tojo A, Okada S, Tokubisa T, Hirai H, Makuuchi M, Hirata Y, Nagai R. Hematopoietic stem cells differentiate into vascular cells that participate in the pathogenesis of atherosclerosis. *Nat Med*. 2002;8:403-409.
17. Simper D, Stalboerger PG, Panetta CJ, Wang S, Caplice NM. Smooth muscle progenitor cells in human blood. *Circulation*. 2002;106:1199-1204.
18. Caplice NM, Bunch TJ, Stalboerger PG, Wang S, Simper D, Miller DV, Russell SJ, Litzow MR, Edwards WD. Smooth muscle cells in human coronary atherosclerosis can originate from cells administered at marrow transplantation. *Proc Natl Acad Sci U S A*. 2003;100:4754-4759.
19. Mrug M, Stopka T, Julian BA, Prchal JF, Prchal JT. Angiotensin II stimulates proliferation of normal early erythroid progenitors. *J Clin Invest*. 1997;100:2310-2314.
20. Rodgers KE, Xiong S, Steer R, diZerega GS. Effect of angiotensin II on hematopoietic progenitor cell proliferation. *Stem Cells*. 2000;18:287-294.
21. Nunes GL, Robinson K, Kalynych A, King SB, 3rd, Sgoutas DS, Berk BC. Vitamins C and E inhibit O<sub>2</sub>-production in the pig coronary artery. *Circulation*. 1997;96:3593-3601.
22. Shi Y, Niculescu R, Wang D, Patel S, Davenpeck KL, Zalewski A. Increased NAD(P)H oxidase and reactive oxygen species in coronary arteries after balloon injury. *Arterioscler Thromb Vasc Biol*. 2001;21:739-745.
23. Lassegue B, Sorescu D, Szocs K, Yin Q, Akers M, Zhang Y, Grant SL, Lambeth JD, Griendling KK. Novel gp91(phox) homologues in vascular smooth muscle cells: nox1 mediates angiotensin II-induced superoxide formation and redox-sensitive signaling pathways. *Circ Res*. 2001;88:888-894.
24. Egashira K. Clinical importance of endothelial function in arteriosclerosis and ischemic heart disease. *Circ J*. 2002;66:529-533.
25. Griendling KK, FitzGerald GA. Oxidative stress and cardiovascular injury: Part II: animal and human studies. *Circulation*. 2003;108:2034-2040.
26. Farb A, Weber DK, Kolodgie FD, Burke AP, Virmani R. Morphological predictors of restenosis after coronary stenting in humans. *Circulation*. 2002;105:2974-2980.
27. Welt FG, Rogers C. Inflammation and restenosis in the stent era. *Arterioscler Thromb Vasc Biol*. 2002;22:1769-1776.
28. Usui M, Egashira K, Ohtani K, Kataoka C, Ishibashi M, Hiasa K, Katoh M, Zhao Q, Kitamoto S, Takeshita A. Anti-monocyte chemoattractant protein-1 gene therapy inhibits restenotic changes (neointimal hyperplasia) after balloon injury in rats and monkeys. *FASEB J*. 2002;16:1838-1840.
29. Egashira K, Zhao Q, Kataoka C, Ohtani K, Usui M, Charo IF, Nishida K, Inoue S, Katoh M, Ichiki T, Takeshita A. Importance of monocyte chemoattractant protein-1 pathway in neointimal hyperplasia after periarterial injury in mice and monkeys. *Circ Res*. 2002;90:1167-1172.
30. Egashira K. Molecular mechanisms mediating inflammation in vascular disease: special reference to monocyte chemoattractant protein-1. *Hypertension*. 2003;41:834-841.
31. Horvath C, Welt FG, Nedelman M, Rao P, Rogers C. Targeting CCR2 or CD18 inhibits experimental in-stent restenosis in primates: inhibitory potential depends on type of injury and leukocytes targeted. *Circ Res*. 2002;90:488-494.
32. Skowasch D, Jabs A, Andrie R, Dinkelbach S, Luderitz B, Bauriedel G. Presence of bone-marrow- and neural-crest-derived cells in intimal hyperplasia at the time of clinical in-stent restenosis. *Cardiovasc Res*. 2003;60:684-691.
33. Takai S, Kim S, Sakonjo H, Miyazaki M. Mechanisms of angiotensin II type 1 receptor blocker for anti-atherosclerotic effect in monkeys fed a high-cholesterol diet. *J Hypertens*. 2003;21:361-369.

# Ovariectomy Augments Hypertension Through Rho-Kinase Activation in the Brain Stem in Female Spontaneously Hypertensive Rats

Koji Ito, Yoshitaka Hirooka, Yoshikuni Kimura, Yoji Sagara, Kenji Sunagawa

**Abstract**—Estrogen protects against increases in arterial pressure (AP) by acting on blood vessels and on cardiovascular centers in the brain. The mechanisms underlying the effects of estrogen in the brain stem, however, are not clear. The aim of the present study was to determine whether ovariectomy affects AP via the Rho/Rho-kinase pathway in the brain stem. We performed bilateral ovariectomy in 12-week-old female spontaneously hypertensive rats. AP and heart rate (HR), measured using radiotelemetry in awake rats, were increased in ovariectomized rats compared with control rats (mean AP:  $163 \pm 3$  versus  $144 \pm 4$  mm Hg; HR:  $455 \pm 4$  versus  $380 \pm 6$  bpm). Continuous intracisternal infusion of Y-27632 significantly attenuated the ovariectomy-induced increase in AP and HR (mean AP:  $137 \pm 6$  versus  $163 \pm 3$  mm Hg; HR:  $379 \pm 10$  versus  $455 \pm 4$  bpm). In addition, we confirmed the increase of Rho-kinase activity in the brain stem in ovariectomized rats, and the increase was attenuated by intracisternal infusion of Y-27632 via the phosphorylated ezrin, radixin, and moesin (ERM) family, which are Rho-kinase target proteins. Furthermore, angiotensin II type 1 receptor expression in the brain stem was significantly greater in ovariectomized rats than in control rats, and the increase was partially reduced by intracisternal infusion of Y-27632. In a separate group of animals, we confirmed that the serum and cerebrospinal fluid  $17\beta$ -estradiol concentrations decreased in ovariectomized rats. These results suggest that depletion of endogenous estrogen by ovariectomy, at least in part, induces hypertension in female spontaneously hypertensive rats via activation of the renin–angiotensin system and the Rho/Rho-kinase pathway in the brain stem. (*Hypertension*. 2006;48:651-657.)

**Key Words:** estrogen ■ brain ■ nervous system, sympathetic ■ receptors, angiotensin ■ blood pressure ■ heart rate

The incidence of cardiovascular diseases is lower in premenopausal women than in age-matched men<sup>1-3</sup> and postmenopausal women.<sup>4</sup> The decreased protective effect against cardiovascular diseases, such as hypertension, in postmenopausal women is thought to be because of endogenous ovarian estrogen depletion. Estrogen decreases arterial pressure through direct effects on blood vessels<sup>5,6</sup> and through effects on central cardiovascular regulatory centers by modulating autonomic function of the cardiovascular system.<sup>7,8</sup> Hormone replacement therapy in postmenopausal women favorably affects cardiovascular regulation by improving baroreflex function and heart rate (HR) variability (HRV)<sup>8</sup> and by decreasing sympathetic nerve activity.<sup>9</sup> In the central nervous system (CNS), endogenous estrogen has numerous effects through estrogen receptor–dependent and -independent pathways.<sup>10,11</sup> Estrogen and estrogen receptors are present in the brain stem where the vasomotor centers, such as the nucleus tractus solitarius (NTS) and the ventrolateral medulla, are located.<sup>12</sup> Medullary injections of exogenous estrogen decrease arterial pressure, HR, and renal sympathetic nerve activity and enhance reflex control of the

HR in male rats, as well as in ovariectomized female rats,<sup>13</sup> suggesting that estrogen has beneficial effects on autonomic functions.<sup>14</sup>

Rho-Kinase is a serine–threonine protein kinase and is one of the effectors of the small GTP-binding protein Rho. This pathway is involved in various cellular functions including smooth muscle contraction, actin cytoskeleton organization, cell proliferation, and cell motility.<sup>15-18</sup> In vascular smooth muscle cells, activation of this pathway contributes to the pathophysiology of hypertension via smooth muscle contraction.<sup>19,20</sup> In the CNS, the Rho/Rho-kinase pathway contributes to the formation of dendritic spines.<sup>21</sup> Dendritic spines form the postsynaptic contact sites of excitatory synapses in the CNS<sup>22</sup> and are thought to be involved in synaptic transmission.<sup>23</sup> We reported previously that Rho-kinase in the brain stem modulates glutamate sensitivity<sup>24</sup> and maintains arterial pressure via the sympathetic nervous system and that activation of the Rho/Rho-kinase pathway might contribute to the central mechanisms of hypertension.<sup>25,26</sup> Estrogen also regulates the formation of excitatory synapses on dendritic spines.<sup>27</sup> Estrogen treatment increases spine number and

Received January 18, 2006; first decision February 6, 2006; revision accepted July 18, 2006.

From the Department of Cardiovascular Medicine, Kyushu University Graduate School of Medical Sciences, Fukuoka, Japan.

Correspondence to Yoshitaka Hirooka, Department of Cardiovascular Medicine, Kyushu University Graduate School of Medical Sciences, 3-1-1 Maidashi, Higashi-ku, Fukuoka 812-8582, Japan. E-mail hyoshi@cardiol.med.kyushu-u.ac.jp

© 2006 American Heart Association, Inc.

*Hypertension* is available at <http://www.hypertensionaha.org>

DOI: 10.1161/01.HYP.0000238125.21656.9e

synaptic density on apical and basal dendrites of CA1 pyramidal neurons in ovariectomized adult female rats.<sup>28,29</sup> These findings led to the hypothesis that the effects of endogenous estrogen on central cardiovascular regulation involve alterations in Rho-kinase activity in the central cardiovascular center. Therefore, the aim of the present study was to determine whether the depletion of endogenous estrogen affects arterial pressure via the Rho/Rho-kinase pathway in the brain stem.

For this purpose, we performed a bilateral ovariectomy in 12-week-old female spontaneously hypertensive rats (SHRs). Y-27632, a specific Rho-kinase inhibitor,<sup>30</sup> was then infused intracisternally for 2 weeks with a miniosmotic pump. Arterial pressure and HR were measured in awake rats using a radiotelemetry system.<sup>31</sup> In a separate group of animals, we confirmed that serum and cerebrospinal fluid (CSF) 17 $\beta$ -estradiol concentrations were decreased in ovariectomized rats. We then compared the Rho-kinase activity in the brain stem between control rats and ovariectomized rats. Finally, we compared the expression level of angiotensin II type 1 receptors (AT1Rs) in the brain stem between control rats and ovariectomized rats, because estrogen functions upstream of the renin-angiotensin system,<sup>32,33</sup> and the Rho/Rho-kinase pathway is downstream of the renin-angiotensin system.<sup>34,35</sup>

## Methods

This study was reviewed and approved by the Committee on the Ethics of Animal Experiments, Kyushu University Graduate School of Medical Sciences, and was conducted according to the Guidelines for Animal Experiments of Kyushu University. Female SHRs (11-week-old, SLC Japan, Hamamatsu, Japan) were used in the present study. A flexible catheter containing an arterial pressure transmitter was introduced into the abdominal aorta just below the renal arteries under sodium pentobarbital (50 mg/kg IP) anesthesia. After surgery, rats were housed singly in cages and allowed unrestricted movement. Rats were fed food devoid of phytoestrogens (AIN 76A, Kyudo Co, Ltd). For 21 days after ovariectomy, arterial pressure and HR were recorded continuously for 10 minutes every other day using a UA-10 telemetry system (Data Sciences International).<sup>25,31</sup>

## Surgical Procedures

Seven days after catheter implantation, we performed bilateral ovariectomy (OVX) or sham operation (control) in the then 12-week-old rats under sodium pentobarbital (50 mg/kg IP) anesthesia. Ovariectomized rats were further randomly divided into 2 groups. The first group received continuous infusion of vehicle (a-CSF, 0.25  $\mu$ L/h; OVX-VEH rats), and the second group received continuous infusion of Y-27632, a specific Rho-kinase inhibitor (5 mmol/L Y-27632, 0.25  $\mu$ L/h; OVX-Y rats), intracisternally for 2 weeks via a miniosmotic pump (Alzet model 1002; Durect Corp). The miniosmotic pump, filled with vehicle or Y-27632, was implanted subcutaneously in the back and connected to a polyethylene tube (PE 10). A small hole was then made in the atlantooccipital membrane, which covers the dorsal surface of the medulla, and the tip of the tube was placed intracisternally and fixed in place with tissue adhesive. After surgery, the rats were free to move about their cages. The infusion was calculated to last 14 days.

## Power Spectral Analysis

To evaluate sympathetic activity, we performed power spectral analysis on day 11 after OVX or sham operation. HR was recorded from 20-minute ECGs performed in awake rats using the radiotelemetry system. The ECG data were calculated using the Powerlab system and Chart 4 software (AD Instruments), and the power spectra of the R-R interval was calculated using the maximum

entropy method with MemCalc software (Suwa Trust Co, Ltd). The frequency bands were adapted for analysis in rats: a very low frequency band (VLF) of 0 to 0.25 Hz, a low frequency band (LF) of 0.25 to 0.8 Hz, and a high frequency band (HF) of 0.8 to 2.4 Hz.<sup>36-38</sup>

## Western Blot Analysis

The animals of each group (control rats, OVX-VEH rats, and OVX-Y rats) were killed with an overdose of sodium pentobarbital on day 11 after OVX or sham operation, and whole brain stem tissues were obtained. The animals used in this experiment were different from those in which arterial pressure, HR, and ECG were monitored. The tissues were obtained as the whole brain stem to ensure that the same areas from each animal were used and then homogenized in lysing buffer containing 40 mmol/L HEPES, 1% Triton X-100, 10% glycerol, 1 mmol/L Na<sub>2</sub>VO<sub>4</sub>, and 1 mmol/L phenylmethylsulfonyl fluoride. The tissue lysate was centrifuged, and the supernatant was collected. The protein concentration was determined using a BCA protein assay kit (Pierce Chemical). A protein aliquot (15  $\mu$ g) from each sample was separated on a 10% sodium dodecyl sulfate-polyacrylamide gel and subsequently transferred onto polyvinylidene difluoride membranes (Immobilon-P membrane, Millipore). Membranes were incubated with rabbit anti-phosphorylated ERM proteins [ezrin (Thr567), radixin (Thr564), and moesin (Thr558)], which are the target proteins of Rho-kinase (this primary antibody was made by Kaibuchi and colleagues<sup>39-42</sup> and has been characterized and used in many previous reports). Membranes were then incubated with a horseradish peroxidase-conjugated horse anti-rabbit IgG antibody (1:10 000). Immunoreactivity was detected by enhanced chemiluminescence autoradiography (ECL Western blotting detection kit, Amersham Pharmacia Biotechnology), and the film was analyzed using NIH Image (developed at the National Institutes of Health and available on the Internet at <http://rsb.info.nih.gov/nih-image/>). Western blot analysis for AT1R was performed as described above using rabbit anti-AT1R antibody (1:1000, Santa Cruz Biotechnology).

## Measurement of Estradiol Concentration in the Serum and CSF

A separate set of 12-week-old female SHRs was divided into 2 groups. In the first group, bilateral OVX alone was performed (OVX rats). In the second group, sham operation was performed (Sham rats). The animals in each group were anesthetized with an overdose of sodium pentobarbital on day 11 after the intervention, and blood samples from the femoral vein were obtained to measure the serum 17 $\beta$ -estradiol concentration by radioimmunoassay performed by SRL Inc). Furthermore, a small hole was made in the atlantooccipital membrane, the tip of a tube connected to a syringe was placed intracisternally, and CSF was collected. Because only a small amount of CSF could be collected from each animal, samples from 5 animals of each group were pooled, and the 17 $\beta$ -estradiol concentration was measured.

## Statistical Analysis

All of the values are expressed as mean  $\pm$  SEM. Two-way ANOVA was used to compare differences in mean arterial pressure (MAP) and HR between the Y-27632 and vehicle infusion groups. Comparisons between any mean values were performed by application of Bonferroni's correction for multiple comparisons. An unpaired *t* test was used to compare the baseline values and the effects of each intervention between groups. Differences were considered to be statistically significant when  $P < 0.05$ .

## Results

### Effects of OVX and Intracisternal Infusion of Y-27632 on Arterial Pressure and HR Measured by Radiotelemetry

The time course of MAP and HR after OVX and intracisternal infusion of Y-27632 is shown in Figure 1. The baseline

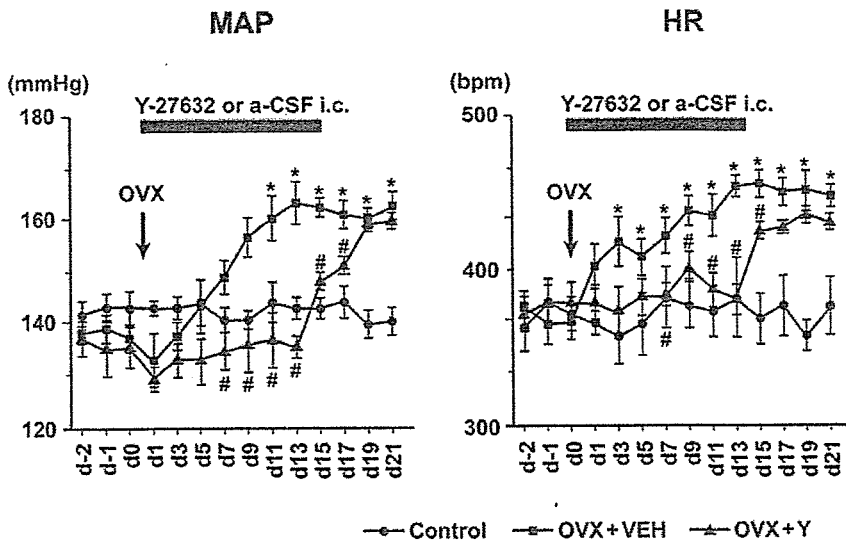


**Figure 1.** Chronic intracisternal infusion of Y-27632. Time course of MAP and HR after ovariectomy with continuous infusion of Y-27632 or vehicle intracisternally for 2 weeks with a miniosmotic pump. MAP and HR were increased in OVX-VEH rats. Y-27632 significantly attenuated the increase in MAP and HR in OVX-Y rats (n=4 for each). \*P<0.05 vs control rats. #P<0.05 vs OVX+VEH rats.

values of arterial pressure in control rats, OVX-VEH rats, and OVX-Y rats were 192±7, 189±9, and 187±7 mm Hg (systolic arterial pressure); 115±3, 113±2, and 112±4 mm Hg (diastolic arterial pressure); and 142±3, 138±2, and 137±3 mm Hg (MAP), respectively. The baseline values of HR in control rats, OVX-VEH rats, and OVX-Y rats were 373±7, 372±6, and 362±7 bpm, respectively. Arterial pressure and HR were significantly increased in OVX-VEH rats. Y-27632 significantly attenuated the increase in arterial pressure and HR in OVX-Y rats. After discontinuing treatment with Y-27632, arterial pressure and HR increased to levels similar to those in OVX-VEH rats. In control rats, arterial pressure and HR did not change after the operation.

**Effects of OVX and Intracisternal Infusion of Y-27632 on HR Power Spectra**

The effects of OVX on HR power spectra are shown in Figure 2. The VLF and LF components were significantly increased in OVX-VEH rats. The VLF and LF components in OVX-Y rats were significantly reduced compared with those in OVX-VEH rats. The HF component, however, did not differ between control rats, OVX-VEH rats, and OVX-Y rats; therefore, the LF/HF ratio, which is considered to be a measure of sympathovagal balance, was also increased in OVX-VEH rats compared with the other groups.

**Western Blot Analysis of Rho-Kinase Activity**

The extent of ERM phosphorylation, which represents Rho-kinase activity, was greater in OVX-VEH rats and in OVX-Y rats than in control rats (Figure 3A). The increase in ERM phosphorylation in OVX-Y rats, however, was significantly less than that in OVX-VEH rats. The expression level of the total ERM family did not differ between groups.

**AT1R Expression Level**

The AT1R expression level was significantly increased in OVX-VEH rats and OVX-Y rats compared with control rats (Figure 3B). The increase in AT1R expression in OVX-Y rats was significantly smaller than that in OVX-VEH rats (Figure 3B).

**Effects of OVX on Serum and CSF Estradiol Concentrations**

On day 11 after the intervention, the serum 17β-estradiol concentration was decreased in OVX rats compared with Sham rats (139±51 pg/mL versus 34±11 pg/mL; n=5 for each; P<0.05). In addition, the CSF 17β-estradiol concentration was also decreased in OVX rats (270.0 pg/mL versus 61.5 pg/mL).

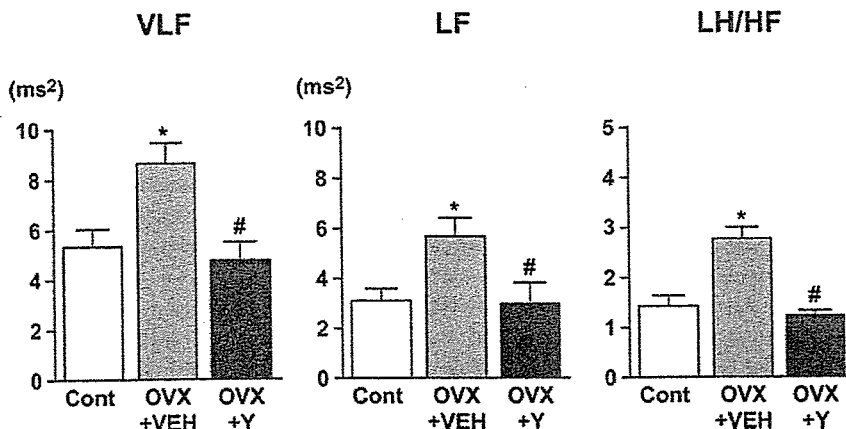


**Figure 2.** Evaluation of sympathetic nerve activity by power spectral analysis. Each graph shows the power density of each spectrum. The power density of VLF and LF reflects sympathetic nerve activity, and the ratio of LF/HF reflects the sympathovagal balance. Both parameters increased in OVX+VEH rats compared with control rats (n=5 for each). \*P<0.05 vs control rats. #P<0.05 vs OVX+VEH rats.

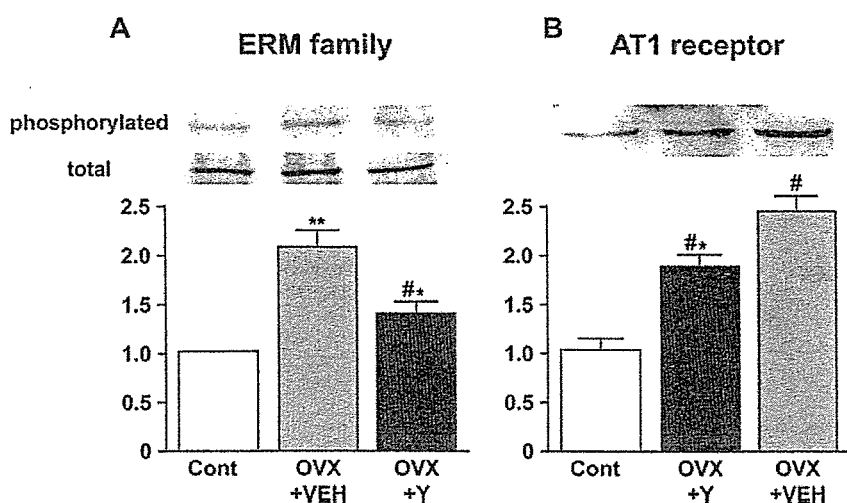


**Figure 3.** A, Western blot analysis demonstrating p-ERM expression in the brain stem. The p-ERM expression level was significantly higher in OVX-VEH rats than in control rats, and its increase was significantly attenuated by Y-27632 infusion. The data are expressed as the relative ratio to controls. The ratio of phosphorylated/total ERM family expression in control rats was assigned a value of 1 ( $n=5$  for each). \*\* $P<0.01$ , \* $P<0.05$  vs control rats. # $P<0.05$  vs OVX+VEH rats. B, Western blot analysis demonstrating AT1R expression in the brain stem. The AT1R expression level was significantly higher in OVX-VEH rats than in control rats, and its increase was significantly attenuated by Y-27632 infusion. The data are expressed as relative ratio to control. The extent of the AT1R in control rats was assigned a value of 1 ( $n=4$  for each). \*\* $P<0.01$ , \* $P<0.05$  vs control rats. # $P<0.05$  vs OVX+VEH rats.

### Discussion

The present study demonstrated that in female SHR, OVX induced an increase in arterial pressure via activation of the sympathetic nervous system, attributable, at least in part, to Rho-kinase activation in the brain stem. Furthermore, the results of the present study suggest that angiotensin II in the brain stem contributes to these mechanisms.

We used only female SHR as a hypertensive model in this study. Previous studies focusing on the interaction between cardiovascular regulation and estrogen demonstrated that OVX has no effect on arterial pressure in normotensive animals.<sup>43,44</sup> Although the Rho-kinase activity and renin-angiotensin system in the brain stem might be affected by OVX in normotensive rats, the effects of OVX, like in postmenopausal women, are more obvious in hypertensive rats than in normotensive rats. Therefore, we used only SHR in the present study. Previous studies also indicated that OVX alters arterial pressure only in salt-sensitive hypertensive models, such as SHR and Dahl salt-sensitive rats.<sup>45–47</sup> There are reports that bilateral OVX in hypertensive rats enhances salt sensitivity but only increases arterial pressure in rats fed a high NaCl diet.<sup>45,46</sup> In the present study, arterial pressure and HR were significantly increased in OVX-VEH rats fed a standard NaCl diet compared with controls from day 7 after bilateral OVX. The discrepant results might be because of differences in age at the time of OVX or in the diet. In fact, rats ovariectomized at a young age and fed a normal diet only have a significant increase in arterial pressure when fed a high-NaCl diet,<sup>45,46</sup> whereas rats ovariectomized at an adult age and fed a phytoestrogen-devoid diet have increased arterial pressure under both a standard NaCl diet and a high-NaCl diet.<sup>47</sup> Furthermore, we measured arterial pressure by radiotelemetry. This system allowed us to measure arterial pressure in awake rats under relatively stress-free conditions compared with other methods, such as the tail-cuff method. In a preliminary study, when we measured arterial pressure by the tail-cuff method, OVX tended to increase arterial pressure, but the difference was not significant (data not shown). These methodologic differences might also cause discrepant results from previous studies. In fact, arterial pressure measured by radiotelemetry is significantly increased in ovariectomized Dahl salt-sensitive rats fed a phytoestrogen-free and low-salt diet.<sup>48</sup>

tomized Dahl salt-sensitive rats fed a phytoestrogen-free and low-salt diet.<sup>48</sup>

Intracisternal infusion of Y-27632 prevented the OVX-induced increase in arterial pressure, suggesting that endogenous Rho-kinase in the brain stem has an important role in OVX-induced hypertension in female SHR. The concentration of Y-27632 (5 mmol/L) used in the present study has selective effects on the CNS.<sup>26</sup> Intracisternal drug infusion affects neurons in several regions of the autonomic cardiovascular area. We demonstrated previously, however, that the Rho/Rho-kinase pathway is activated in the NTS of SHR but not normotensive rats, and Rho-kinase inhibition in the NTS induces a significant reduction in arterial pressure.<sup>25</sup> In addition, the NTS is positioned at the dorsal surface of the medulla. Therefore, Y-27632 might have greater effects on neurons of the NTS than on neurons of other nuclei, although we cannot exclude the possibility that it affects other autonomic areas in the brain stem. Together, these findings suggest that the effect of Y-27632 is mediated in part by the inhibition of Rho-kinase activity in the NTS.

In the present study, it is unlikely that the results are because of nonspecific effects caused by the surgical procedure, because continuous intracisternal infusion of vehicle using the same device did not suppress the increase in arterial pressure, and after discontinuing the Y-27632 infusion, arterial pressure increased to levels similar to those in OVX-VEH rats. In addition, ERM phosphorylation in the brain stem was significantly increased in OVX-VEH rats and reduced in OVX-Y rats, which strongly suggests that the Rho-kinase activity in the brain stem of OVX-VEH rats was increased and that Y-27632 suppressed Rho-kinase activity. We estimated the extent of ERM phosphorylation as a marker of Rho-kinase activity. The ERM family members are concentrated in the actin-rich cell surface, cross-link actin filaments with the plasma membrane, and contribute to cell-cell adhesion and maintenance of cell shape and cell motility.<sup>49</sup> Although the role of ERM family members in the central cardiovascular regulation is not clear, and ERM family members might be the substrates of other kinases, ERM phosphorylation is commonly used as an indicator of Rho-kinase activity.<sup>25,26,34,40–42</sup>



In the present study, intracisternal infusion of Y-27632 nearly abolished the OVX-induced increase in arterial pressure. We reported previously that Rho-kinase activity in the brain stem of hypertensive rats is increased compared with normotensive rats.<sup>25,26</sup> Therefore, intracisternal infusion of Y-27632 might suppress not only the OVX-induced increase in Rho-kinase activity but also basal Rho-kinase activity, thereby inducing a greater reduction in arterial pressure than that induced by OVX. In most previous studies, arterial pressure changes were evaluated several weeks after OVX. In the present study,  $\approx 1$  week after OVX, arterial pressure of ovariectomized rats was significantly increased compared with that of control rats. As mentioned above, we used more sensitive methods for measuring arterial pressure. In addition, we confirmed that the  $17\beta$ -estradiol concentration, both in the serum and the CSF, decreased by  $\approx 25\%$  at 11 days after OVX. Although the serum and the CSF estradiol concentrations were markedly decreased by OVX, the concentrations were still high. We speculate that other organs, such as adrenal glands or adipocytes, produced estradiol after OVX. We did not address these issues, however, and do not have precise interpretations for this finding. In the present study, we primarily wanted to confirm that OVX reduced serum and CSF estradiol concentrations.

We estimated sympathetic activity using the HRV power spectral analysis. HRV is used as a noninvasive marker of autonomic outflow to the heart in a variety of disease states.<sup>50</sup> HRV has a very specific pattern in the frequency domains delineated by the HF, LF, and VLF components.<sup>36</sup> Spontaneous VLF power, which is 0 to 0.25 Hz, and LF power, which is 0.25 to 0.8 Hz, in the rat are particularly related to sympathetic nerve activity.<sup>36–38</sup> In fact, an increased LF component in R–R variability occurs in various conditions known to decrease baroreflex gain and increase sympathetic outflow, such as tilt, mental stress, and exercise.<sup>51</sup> On the other hand, the HF component is attributed to vagal and respiratory control, and the LF/HF ratio is used as an index of sympathovagal balance.<sup>52</sup> Therefore, we also used spectral analysis of the HR in the present study. The VLF and LF powers or the LF/HF ratio were greater in OVX-VEH rats than in control rats, and those in OVX-Y rats were significantly reduced compared with OVX-VEH rats. Furthermore, the HR increase could also be an indicator of activation of the sympathetic nervous system. In the present study, HR was greater in OVX-VEH rats than in control rats and that in OVX-Y rats was significantly reduced compared with OVX-VEH rats. These results indicate that sympathetic activity was increased by OVX, and intracisternal infusion of Y-27632 significantly attenuated the increase in sympathetic activity.

Estrogen decreases arterial pressure by acting on blood vessels or the kidney via the AT1R.<sup>5,6,41</sup> Furthermore, the renin–angiotensin system is also a major pathway of the central mechanisms of hypertension. Previous reports suggest that angiotensin II contributes to the neural mechanisms of hypertension.<sup>53,54</sup> In addition, inhibition of Rho-kinase activity suppresses angiotensin II–induced cardiovascular effects.<sup>34</sup> Therefore, we examined AT1R expression levels in each group to address the possibility of a partial interaction between the renin–angiotensin system and the Rho/Rho-

kinase pathway in OVX-induced hypertension. The AT1R levels in the brain stem were significantly increased by OVX, and this increase was attenuated by intracisternal infusion of Y-27632. These results suggested that angiotensin II in the brain stem contributes to the mechanisms of OVX-induced hypertension in female SHR. The Rho/Rho-kinase pathway is downstream of the renin–angiotensin system.<sup>34,35</sup> RhoA regulates the expression of AT1R,<sup>55</sup> however, and Y-27632 inhibits not only Rho-kinase activity, but also RhoA activity.<sup>56</sup> Therefore, Y-27632 might attenuate RhoA activity by direct effects or negative feedback mechanisms of the Rho/Rho-kinase pathway and, thus, lead to the inhibition of AT1R expression. The finding that Y-27632 had only a weak effect on AT1R expression, together with the results of previous studies,<sup>34,35</sup> suggest that the depletion of endogenous estrogen activates the Rho/Rho-kinase pathway in the brain stem and might also activate the renin–angiotensin system.

In conclusion, we demonstrated that the depletion of endogenous estrogen by OVX increases arterial pressure in female SHR, at least in part, via activation of the renin–angiotensin system and Rho/Rho-kinase pathway in the brain stem.

### Perspectives

It is not known how OVX induces increases in arterial pressure in female SHR. In the CNS, both the Rho/Rho-kinase pathway and estrogen regulate the formation of excitatory synapses on dendritic spines.<sup>27</sup> Dendritic spines form the postsynaptic contact sites of excitatory synapses in the CNS<sup>22</sup> and are associated with glutamate sensitivity.<sup>23</sup> Therefore, estrogen depletion might induce morphological or functional changes in the dendritic spines via Rho-kinase activation. On the other hand, estrogen depletion increases arterial pressure and hypothalamic norepinephrine levels,<sup>46</sup> and hypothalamus neurons project to the dorsomedial medulla neurons, such as those in the NTS.<sup>57</sup> These findings suggest that estrogen depletion affects dorsomedial medulla neurons via changes in the hypothalamic norepinephrine levels. Although further studies are needed to clarify the mechanisms of these effects, the Rho/Rho-kinase pathway in the brain stem might be involved in the mechanisms underlying OVX-induced hypertension, because Rho-kinase in the NTS is involved in central mechanisms of cardiovascular regulation via modulation of the sensitivity of NTS neurons to glutamate.<sup>24–26,58</sup>

### Sources of Funding

This study was supported by Grants-in-Aid for Scientific Research from the Japan Society for the Promotion of Science (S18659230, A15200040, C17590745), and by a Grant for Research on the Autonomic Nervous System and Hypertension from Kimura Memorial Heart Foundation/Pfizer Pharmaceuticals, Inc.

### Disclosures

None.

### References

- Hayes SN, Taler SJ. Hypertension in women: current understanding of gender difference. *Mayo Clin Proc.* 1998;73:157–165.
- Khoury S, Yarrows SA, O'Brien TK, Sowers J. Ambulatory blood pressure monitoring in nonacademic setting: effects of age and sex. *Am J Hypertens.* 1992;5:616–623.

3. Wiinber N, Hoegholm A, Benzton MWE. 24-Hr ambulatory blood pressure in 352 normal Danish subjects related to age and gender. *Am J Hypertens*. 1995;8:978–986.
4. Kannel WB, Wilson PW. Risk factors that attenuate the female coronary disease advantage. *Arch Intern Med*. 1995;155:57–61.
5. Dubey RK, Oparil S, Inthurn B, Jackson EK. Sex hormones and hypertension. *Cardiovasc Res*. 2002;53:688–708.
6. Mendelsohn ME, Karas RH. The protective effects of estrogen on the cardiovascular system. *N Engl J Med*. 1999;340:1801–1811.
7. Pamidimukkala J, Taylor JA, Welshons WV, Lubahn DB, Hay M. Estrogen modulation of baroreflex function in conscious mice. *Am J Physiol*. 2003;284:R983–R989.
8. Huikuri HV, Pikkujamsa SM, Airaksinen J, Ikaheimo MJ, Rantala AO, Kauma H, Lilja M, Kesaniemi A. Sex-related differences in autonomic modulation of heart rate in middle-aged subjects. *Circulation*. 1996;94:122–125.
9. Vongpatanasin W, Tuncel M, Mansour Y, Arbique D, Victor RG. Transdermal estrogen replacement therapy decreases sympathetic activity in postmenopausal women. *Circulation*. 2001;103:2903–2908.
10. McEwen BS, Alves SE. Estrogen action in the central nervous system. *Endocr Rev*. 1999;20:279–307.
11. Blaustein JD, Lehman MN, Turcotte JC, Greene G. Estrogen receptors in dendrites and axon terminals in guinea pig hypothalamus. *Endocrinology*. 1992;131:281–290.
12. Haywood SA, Simonian SX, van der Beek EM, Bicknell RJ, Herrison AE. Fluctuating estrogen and progesterone receptor expression in brainstem norepinephrine neurons through the rat estrous cycle. *Endocrinology*. 1999;140:3255–3263.
13. Saleh MC, Connell BJ, Saleh TM. Autonomic and cardiovascular reflex responses to central estrogen injection in ovariectomized female rats. *Brain Res*. 2000;879:105–114.
14. Saleh MC, Connell BJ, Saleh TM. Medullary and intrathecal injections of 17 $\beta$ -estradiol in male rats. *Brain Res*. 2000;867:200–209.
15. Kimura K, Ito M, Amano M, Chihara K, Fukata Y, Nakafuku M, Yamamori B, Feng J, Nakano T, Okawa K, Iwamatsu A, Kaibuchi K. Regulation of myosin phosphatase by Rho and Rho-associated kinase (Rho-kinase). *Science*. 1996;273:245–248.
16. Kawano Y, Fukata Y, Oshiro N, Amano M, Nakamura T, Ito M, Matsumura F, Inagaki M, Kaibuchi K. Phosphorylation of myosin binding subunit(MBS) of myosin phosphatase by Rho-kinase in vivo. *J Cell Biol*. 1999;147:1023–1037.
17. Shimokawa H. Rho-kinase as a novel therapeutic target in treatment of cardiovascular disease. *J Cardiovasc Pharmacol*. 2002;39:319–327.
18. Loirand G, Guérin P, Pacaud P. Rho kinase in cardiovascular physiology and pathophysiology. *Circ Res*. 2006;98:322–334.
19. Mukai Y, Shimokawa H, Matoba T, Kandabashi T, Satoh S, Hiroki J, Kaibuchi K, Takeshita A. Involvement of Rho-kinase in hypertensive vascular disease: a novel therapeutic target in hypertension. *FASEB J*. 2001;15:1062–1064.
20. Masumoto A, Hirooka Y, Shimokawa H, Hironaga K, Setoguchi S, Takeshita A. Possible involvement of Rho-kinase in the pathogenesis of hypertension in humans. *Hypertension*. 2001;38:1307–1310.
21. Nakayama AY, Harms MB, Luo L. Small GTPases Rac and Rho in the maintenance of dendritic spines and branches in hippocampal pyramidal neurons. *J Neurosci*. 2000;20:5329–5338.
22. Koch C, Zador A. The function of dendritic spines: devices subserving biochemical rather than electrical compartmentalization. *J Neurosci*. 1993;13:413–422.
23. Matsuzaki M, Ellis-Davies GC, Nemoto T, Miyashita Y, Iino M, Kasai H. Dendritic spine geometry is critical for AMPA receptor expression in hippocampal CA1 pyramidal neurons. *Nat Neurosci*. 2001;4:1086–1092.
24. Ito K, Hirooka Y, Hori N, Kimura Y, Sagara Y, Shimokawa H, Takeshita A, Sunagawa K. Inhibition of Rho-kinase in the nucleus tractus solitarius enhances glutamate sensitivity in rats. *Hypertension*. 2005;46:360–365.
25. Ito K, Hirooka Y, Sakai K, Kishi T, Kaibuchi K, Shimokawa H, Takeshita A. Rho/Rho-kinase pathway in brain stem contributes to blood pressure regulation via sympathetic nervous system. *Circ Res*. 2003;92:1337–1343.
26. Ito K, Hirooka Y, Kishi T, Kimura Y, Kaibuchi K, Shimokawa H, Takeshita A. Rho/Rho-kinase pathway in the brainstem contributes to hypertension caused by chronic nitric oxide synthase inhibition. *Hypertension*. 2004;43:156–162.
27. McEwen BS, Tanapat P, Weiland NG. Inhibition of dendritic spine induction on hippocampal CA1 pyramidal neurons by a nonsteroidal estrogen antagonist in female rats. *Endocrinology*. 1999;140:1044–1047.
28. Gould E, Woolley C, Frankfurt M, McEwen BS. Gonadal steroids regulate dendritic spine density in hippocampal pyramidal cells in adulthood. *J Neurosci*. 1990;10:1286–1291.
29. Woolley C, McEwen BS. Roles of estradiol and progesterone in regulation of hippocampal dendritic spine density during the estrous cycle in the rat. *J Comp Neurol*. 1993;336:293–306.
30. Uehata M, Ishizaki T, Satoh H, Ono T, Kawahara T, Morishita, Tamakawa H, Yamagami K, Inui J, Maekawa M, Narumiya S. Calcium sensitization of smooth muscle mediated by a Rho-associated protein kinase in hypertension. *Nature*. 1997;389:990–994.
31. Sakai K, Hirooka Y, Matsuo I, Eshima K, Shigematsu H, Shimokawa H, Takeshita A. Overexpression of eNOS in NTS causes hypotension and bradycardia in vivo. *Hypertension*. 2000;36:1023–1028.
32. Gragasin FS, Xu Y, Arenas IA, Kainth N, Davidge ST. Estrogen reduces angiotensin II-induced nitric oxide synthase and NAD(P)H oxidase expression in endothelial cells. *Arterioscler Thromb Vasc Biol*. 2003;23:38–44.
33. Gallagher PE, Li P, Lenhart JR, Chappell MC, Brosnihan KB. Estrogen regulation of angiotensin-converting enzyme mRNA. *Hypertension*. 1999;33[part II]:323–328.
34. Higashi M, Shimokawa H, Hattori T, Hiroki J, Mukai Y, Morikawa K, Ichiki T, Takahashi S, Takeshita A. Long-term inhibition of Rho-kinase suppresses angiotensin II-induced cardiovascular hypertrophy in rats in vivo. Effect on endothelial NAD(P)H oxidase system. *Circ Res*. 2003;93:767–775.
35. Funakoshi Y, Ichiki T, Shimokawa H, Egashira K, Takeda K, Kaibuchi K, Takeya M, Yoshimura T, Takeshita A. A critical role of Rho-kinase in angiotensin II-induced monocyte chemoattractant protein-1 expression in rat vascular smooth muscle cells. *Hypertension*. 2001;38:100–104.
36. Kuo TBJ, Yang CCH. Altered frequency characteristic of central vasomotor control in SHR. *Am J Physiol*. 2000;278:H201–H207.
37. Cerutti C, Barres C, Paultre C. Baroreflex modulation of blood pressure and heart rate variabilities in rats: assessment by spectral analysis. *Am J Physiol*. 1994;266:H1993–H2000.
38. Cerutti C, Gustin MP, Paultre M, Julien LC, Vincent JM, Sassard J. Autonomic nervous system and cardiovascular variability in rats: a spectral analysis approach. *Am J Physiol*. 1991;261:H1291–H1299.
39. Matsui T, Maeda M, Doi Y, Yonemura S, Amano M, Kaibuchi K, Tsukita S. Rho-kinase phosphorylates COOH-terminal threonines of Ezrin/Radixin/Moesin (ERM) proteins and regulates their head-to-tail association. *J Cell Biol*. 1998;140:647–657.
40. Morishige K, Shimokawa H, Eto Y, Kandabashi T, Miyata K, Matsumoto Y, Hoshijima M, Kaibuchi K, Takeshita A. Adenovirus-mediated transfer of dominant-negative Rho-kinase induces a regression of coronary arteriosclerosis in pigs in vivo. *Arterioscler Thromb Vasc Biol*. 2001;21:548–554.
41. Takemoto M, Sun J, Hiroki J, Shimokawa H, Liao JK. Rho-kinase mediates hypoxia-induced downregulation of endothelial nitric oxide synthase. *Circulation*. 2002;106:57–62.
42. Matsumoto Y, Uwatoku T, Oi K, Abe K, Hattori T, Morishige K, Eto Y, Fukumoto Y, Nakamura K, Shibata Y, Matsuda T, Takeshita A, Shimokawa H. Long-term inhibition of Rho-kinase suppresses neointimal formation after stent implantation in porcine coronary arteries: involvement of multiple mechanisms. *Arterioscler Thromb Vasc Biol*. 2004;24:181–186.
43. Mohamed MK, El-Mas MM, Abdel AA. Estrogen enhancement of baroreflex sensitivity is centrally mediated. *Am J Physiol*. 1999;276:R1030–R1037.
44. Pamidimukkala J, Taylor JA, Welshons WV, Lubahn DB, Hay M. Estrogen modulation of baroreflex function in conscious mice. *Am J Physiol*. 2003;284:R983–R989.
45. Harrison-Bernard LM, Schulman IH, Raj L. Postovariectomy hypertension is linked to increased renal AT1 receptor and salt sensitivity. *Hypertension*. 2003;42:1157–1163.
46. Fang Z, Carlson SH, Chen YF, Oparil S, Wyss JM. Estrogen depletion induces NaCl-sensitive hypertension in female spontaneously hypertensive rats. *Am J Physiol*. 2001;281:R1934–R1939.
47. Peng N, Clark JT, Wei C-C, Wyss JM. Estrogen depletion increases blood pressure and hypothalamic norepinephrine in middle-aged spontaneously hypertensive rats. *Hypertension*. 2003;41:1164–1167.
48. Hinojosa-Laborde C, Craig T, Zheng W, Ji H, Haywood JR, Sandberg K. Ovariectomy augments hypertension in aging female dahl salt-sensitive rats. *Hypertension*. 2004;44:405–409.
49. Louvet-Vallée S. ERM proteins: From cellular architecture to cell signaling. *Biol Cell*. 2000;92:305–316.

50. Task Force of the European Society of Cardiology and the North Am Society of Pacing and Electrophysiology. Heart rate variability. Standards of measurement, physiological interpretation, and clinical use. *Eur Heart J*. 1996;17:354–381.
51. Lanfranchi PA, Somers VK. Arterial baroreflex function and cardiovascular variability: interactions and implications. *Am J Physiol*. 2002;283:R815–R826.
52. Pagani M, Lombardi F, Guzzetti S, Rimoldi O, Furlan R, Pizzinelli P, Sandrone G, Malfatto G, Dell’Orto S, Piccaluga E. Power spectral analysis of heart rate and arterial pressure variabilities as a marker of sympatho-vagal interaction in man and conscious dog. *Circ Res*. 1986;59:178–193.
53. Matsumura K, Averill DB, Ferrario CM. Angiotensin II acts at AT1 receptors in the nucleus of the solitary tract to attenuate the baroreceptor reflex. *Am J Physiol*. 1998;275:R1611–R1619.
54. Eshima K, Hirooka Y, Shigematsu H, Matsuo I, Koike G, Sakai K, Takeshita A. Angiotensin in the nucleus tractus solitarii contributes to neurogenic hypertension caused by chronic nitric oxide synthase inhibition. *Hypertension*. 2000;36:259–263.
55. Ichiki T, Takeda K, Tokunou T, Iino N, Egashira K, Shimokawa H, Hirano K, Kanaide H, Takeshita A. Downregulation of angiotensin II type 1 receptor by hydrophobic 3-hydroxy-3-methylglutaryl coenzyme A reductase inhibitors in vascular smooth muscle cells. *Arterioscler Thromb Vasc Biol*. 2001;21:1896–1901.
56. Kobayashi N, Nakano S, Mita S, Kobayashi T, Honda T, Tsubokou Y, Matsuoka H. Involvement of Rho-kinase pathway for angiotensin II-induced plasminogen activator inhibitor-1 gene expression and cardiovascular remodeling in hypertensive rats. *J Pharmacol Exp Therap*. 2002;301:459–466.
57. Nishimura H, Oomura Y. Effects of hypothalamic stimulation on activity of dorsomedial medulla neurons that respond to subdiaphragmatic vagal stimulation. *J Neurophysiol*. 1987;58:655–675.
58. Ito K, Hirooka Y, Sagara Y, Kimura Y, Kaibuchi K, Shimokawa H, Takeshita A, Sunagawa K. Inhibition of Rho-kinase in the brainstem augments baroreflex control of heart rate in rats. *Hypertension*. 2004;44:478–483.

## Telmisartan downregulates angiotensin II type 1 receptor through activation of peroxisome proliferator-activated receptor $\gamma$

Ikuyo Imayama, Toshihiro Ichiki\*, Keita Inanaga, Hideki Ohtsubo, Kae Fukuyama, Hiroki Ono, Yasuko Hashiguchi, Kenji Sunagawa

Department of Cardiovascular Medicine, Kyushu University Graduate School of Medical Sciences, 3-1-1 Maidashi, Higashi-ku, 812-8582 Fukuoka, Japan

Received 2 May 2006; received in revised form 4 July 2006; accepted 6 July 2006

Available online 21 July 2006

Time for primary review 26 days

### Abstract

**Objective:** Telmisartan, an angiotensin II type 1 receptor (AT1R) antagonist, was found to have a unique property: it is a partial agonist of peroxisome proliferator-activated receptor gamma (PPAR $\gamma$ ). Since previous studies have demonstrated that PPAR $\gamma$  activators suppressed AT1R expression, we examined whether telmisartan affects AT1R expression in vascular smooth muscle cells.

**Methods:** Vascular smooth muscle cells were derived from the thoracic aorta of Wistar–Kyoto rat. Northern and Western blotting analysis were used to examine AT1R mRNA and protein expression, respectively. The DEAE-dextran method was used for transfection, and the promoter activity of AT1R was examined by luciferase assay.

**Results:** Telmisartan decreased the expression of AT1R at the mRNA and protein levels in a dose- and time-dependent manner. Decreased AT1R promoter activity with unchanged mRNA stability suggested that telmisartan suppressed AT1R gene expression at the transcriptional level. However, the expression of AT1R was not suppressed by other AT1R antagonists such as candesartan or olmesartan. Since the suppression of AT1R expression was prevented by pretreatment with GW9662, a PPAR $\gamma$  antagonist, PPAR $\gamma$  should have participated in the process. The deletion and mutation analysis of the AT1R gene promoter indicated that a GC box located in the proximal promoter region is responsible for the telmisartan-induced downregulation.

**Conclusion:** Our data provides a novel insight into an effect of telmisartan: telmisartan inhibits AT1R gene expression through PPAR $\gamma$  activation. The dual inhibition of angiotensin II function by telmisartan – AT1R blockade and downregulation – would contribute to more complete inhibition of the renin–angiotensin system.

© 2006 European Society of Cardiology. Published by Elsevier B.V. All rights reserved.

**Keywords:** Antihypertensive; Diuretic drugs; Atherosclerosis; Gene expression; Receptors; Renin–angiotensin system

### 1. Introduction

Angiotensin (Ang) II is a main final effector molecule of the renin–angiotensin system. Physiologically, Ang II plays an important role in controlling the blood pressure and the fluid volume [1]. However, Ang II is also involved in pathological conditions such as renal insufficiency [2], cardiovascular diseases [3] and metabolic disorders [4].

The effect of Ang II are mediated by Ang II receptors and so far two isoforms, type 1 receptor (AT1R) and type 2

receptor (AT2R), have been identified [5]. AT1R mediates most of the traditional effects of Ang II such as vasoconstriction, sodium retention, aldosterone secretion, and cell proliferation [1]. In contrast, AT2R mediates vasodilation and growth inhibition that opposes to the effects of AT1R [6]. However, it was reported that AT2R was hardly detected in blood vessel of adult animal [6].

Ang I converting enzyme inhibitors and AT1R antagonists are clinically used. Many clinical trials have demonstrated that these drugs are beneficial in the treatment of heart failure, renal failure and myocardial infarction. These drugs are also useful in preventing new-onset diabetes mellitus [7] and atrial fibrillation [8]. Telmisartan (Tel), one of the clinically

\* Corresponding author. Tel.: +81 92 642 5361; fax: +81 92 642 5374.  
E-mail address: ichiki@cardiol.med.kyushu-u.ac.jp (T. Ichiki).

available AT1R antagonists, was recently reported to have a partial agonistic effect on peroxisome proliferator activated receptor gamma (PPAR $\gamma$ ) [9,10]. PPAR $\gamma$  is a nuclear receptor that regulates specific gene transcription [11]. The target genes of PPAR $\gamma$  are involved in the regulation of lipid and glucose metabolism [12], and inflammatory responses. Moreover, several studies have demonstrated that PPAR $\gamma$  activators are effective in preventing atherogenesis [13,14]. Therefore, Tel is focused for its additional therapeutic values in patients with metabolic disorders.

Previously, we and another group reported that activators of PPAR $\gamma$  such as 15-deoxy- $\Delta^{12,14}$ -prostaglandin J<sub>2</sub> and pioglitazone (Pio) decreased the expression of AT1R in vascular smooth muscle cells (VSMCs) [15,16]. We, therefore, examined whether Tel, a partial agonist of PPAR $\gamma$ , affects the expression of AT1R in a similar way to PPAR $\gamma$  agonists in VSMCs.

## 2. Materials and methods

### 2.1. Materials

Tel and olmesartan (Olm) were generous gifts from Boehringer Ingelheim Co. and Sankyo Co., respectively. Candesartan (Can) and Pio were provided by Takeda Pharmaceutical Company. Dulbecco's modified Eagle's medium (DMEM) and fetal bovine serum (FBS) were purchased from GIBCO BRL. Bovine serum albumin (BSA) and Actinomycin D (ActD) were purchased from Sigma Chemical Co. Rabbit polyclonal antibody against AT1R [17,18] and  $\alpha$ -tubulin were from Santa Cruz Biotechnology. Mouse polyclonal antibody against pERK and rabbit polyclonal antibody against ERK were from Cell Signaling Technology, Inc. Horseradish peroxidase-conjugated secondary antibodies (anti-rabbit IgG and anti-mouse IgG) were purchased from VECTOR Laboratories Inc. [ $\alpha$ -<sup>32</sup>P] dCTP was purchased from Perkin-Elmer Life Sciences.

### 2.2. Cell culture

All procedures and care of the animals were approved by the Committee on Ethics of Animal Experiments, Kyushu University and this study conforms with the Guide for the Care and Use of Laboratory Animals published by the US National Institutes of Health (NIH Publication No. 85-23, revised 1996). VSMCs were isolated from the thoracic aorta of Wistar-Kyoto rat by an explant method and maintained in DMEM supplemented with 10% FBS at 37 °C in a humidified atmosphere of 95% air–5% CO<sub>2</sub>. VSMCs were cultured until grown to confluence, cultured in DMEM with 0.1% BSA for additional 2 days and used in the experiment. Cells between passages 4 and 14 were used.

### 2.3. Northern blotting

Total RNA was prepared by acid guanidinium thiocyanate–phenol–chloroform extraction method [19]. Total RNA was electrophoresed on a 1.0% agarose, 1.0% formaldehyde

gel, transferred to Hybond-N+ membrane (Amersham Biosciences) by a capillary transfer method in 10 $\times$  SSC (1 $\times$  SSC is 150 mmol/L of sodium and 15 mmol/L of sodium citrate) buffer overnight. The membrane was cross-linked by a UV cross-linker (Funakoshi Corporation). Prehybridization and hybridization were performed in a buffer containing 50% formamide, 5 $\times$  SSC, 80 mmol/L sodium phosphate (pH 7.5), 2 $\times$  Denhardt's Solution, 1% SDS, and 100  $\mu$ g/L of heat-denatured salmon sperm DNA for 1 h and 16 h, respectively, at 42 °C. An ECORI fragment of the third exon of rat AT1A gene [20] and ribosomal RNA were labeled with <sup>32</sup>P by a Random Primer DNA Labeling Kit Ver.2 (Takara Bio Inc.) and used as a probe after heat denaturation. The hybridized membrane was washed twice with 2 $\times$  SSC at room temperature, followed by two washes with 2 $\times$  SSC/1% SDS for 30 min at 55 °C. The membrane was then exposed to a KODAK BioMax XAR Film at –80 °C. The hybridized membrane was stripped by boiling in 0.5% SDS solution and hybridized to a <sup>32</sup>P-labeled ribosomal RNA probe to obtain reference for the amount of applied RNA. Autoradiography was scanned and analyzed by a MacBAS Bioimage Analyzer (Fuji Photo Film Co). To analyze mRNA stability of AT1R, Actinomycin (Act) D (5  $\mu$ g/mL) was added after 6 h of stimulation with Tel (10  $\mu$ mol/L). In a control experiment, only ActD was added. Cells were harvested after 3, 6, 12, and 24 h of addition of ActD and expression level of AT1R mRNA was examined by Northern blot analysis.

### 2.4. Measurement of AT1R gene promoter activity

Five deletion mutants of AT<sub>1A</sub> gene promoter were prepared by digestion with restriction endonucleases and

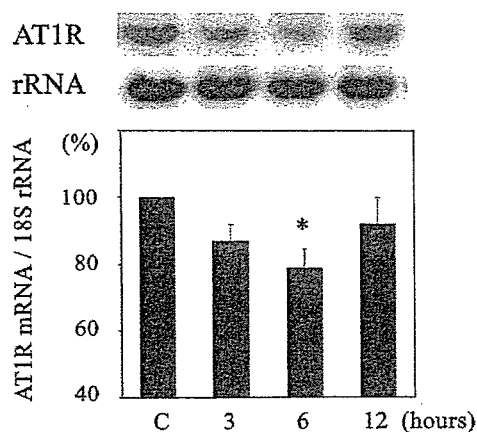


Fig. 1. Telmisartan (Tel) suppressed AT1R mRNA expression in VSMCs. VSMCs were incubated with Tel (10  $\mu$ mol/L) for various periods as indicated in the figure. Total RNA was isolated and expression of AT1R mRNA and 18S rRNA (rRNA) was determined by Northern blot analysis. Radioactivity of AT1R mRNA was measured with an imaging analyzer and was normalized by radioactivity of rRNA. Values (mean $\pm$ S.E.M.) are expressed as a percent of control culture in the bar graph (100%) ( $n=5$ ). \* $P<0.05$  vs control (c).

ligated to luciferase gene [21]. Confluent VSMCs were split by trypsin/EDTA solution and cells were prepared in a 6 cm tissue culture dish. At 80% confluence, 5  $\mu\text{g}$  of AT1 promoter-luciferase fusion DNA and 2  $\mu\text{g}$  of  $\beta$ -galactosidase gene were introduced to VSMC by the DEAE-dextran method according to the manufacturer's instruction (Promega Corporation). The cells were cultured in DMEM with 10% FBS for 18 h, washed twice with phosphate buffered saline, cultured in DMEM with 0.1% BSA for 24 h and stimulated with Tel (10  $\mu\text{mol/L}$ ) for 12 h. Then, the cells were lysed in 200  $\mu\text{L}$  of Reporter lysis buffer (Promega Corporation). 100  $\mu\text{L}$  of lysate was used for luciferase activity assay in a Lumat luminometer (LB 9501, Berthold, Germany). The  $\beta$ -galactosidase activity in the same sample was measured spectrophotometrically according to Sambrook et al. [22] and used to normalize the luciferase activity.

The AT1R promoter-luciferase construct with mutation in the GC-box-related sequence (wild type: TGCAGAGCAGC GACGCCCCCTAGGC mutant: TGCAGAGCAGCGA CGTTTCCTAGGC) was a generous gift from Dr. Sugawara (Tohoku University) [16].

### 2.5. Western blot analysis

VSMCs were lysed in a lysis buffer containing RIPA (100 mM sodium, 60 mM  $\text{Na}_2\text{HPO}_4$ , 100 mM NaF 10 mM EDTA, and 20 mM Tris), 1% aprotinin, 0.5% pepstatin A, 1 mmol/L PMSF, and 0.05% leupeptin. Protein concentrations were determined with the bicinchoninic acid protein assay kit (Pierce Chemical Co). Cell lysates were heated in a sample buffer (62.5 mmol/L Tris-HCl [pH 6.8], 10% glycerol, 2% SDS, 0.05% bromophenolblue, and

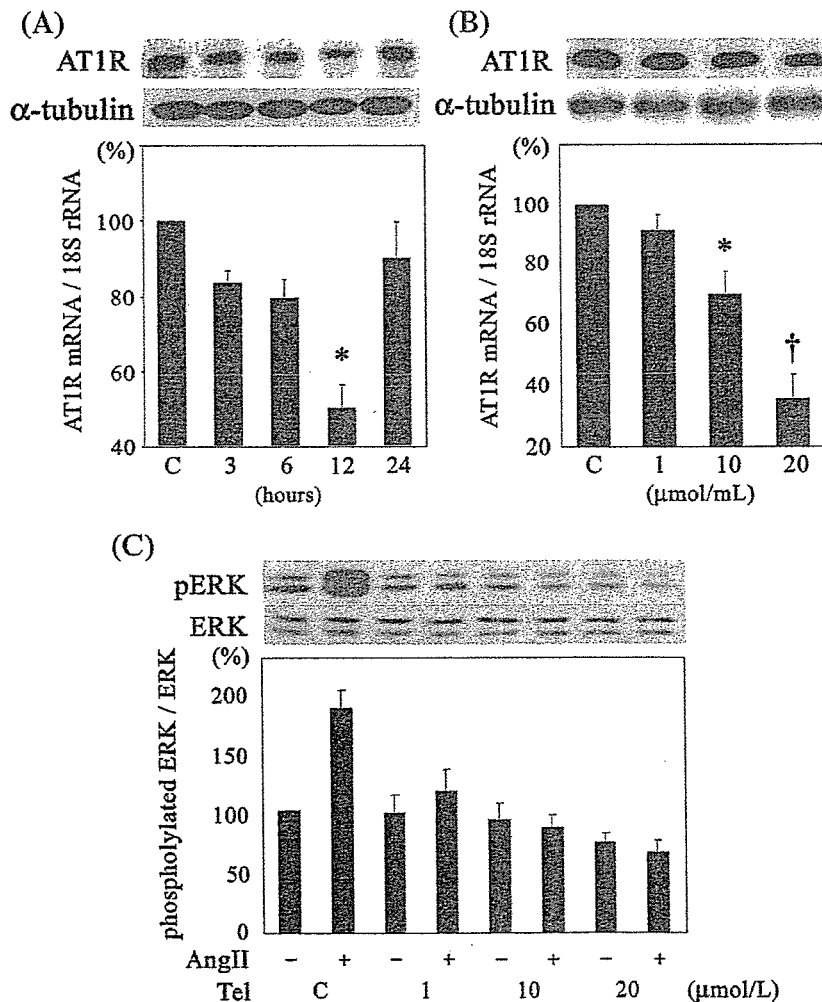


Fig. 2. Suppression of AT1R protein by telmisartan (Tel) in VSMCs. (A) VSMCs were incubated with Tel (10  $\mu\text{mol/L}$ ) for various periods as indicated in the figure. (B) VSMCs were incubated with Tel at concentrations varying from 1 to 20  $\mu\text{mol/L}$  for 12 h. Expression of AT1R protein and  $\alpha$ -tubulin was detected by Western blot analysis. The density of the specific band was scanned and quantified with an imaging analyzer. The ratio of AT1R to  $\alpha$ -tubulin is shown in the bar graph. (C) VSMCs were incubated with Tel at various concentrations as indicated in the figure and stimulated by Ang II (100  $\mu\text{mol/L}$ ). Expressions of pERK and ERK protein were detected by Western blot analysis. The density of the specific band was scanned and quantified with an imaging analyzer. The ratio of pERK to ERK is shown in the bar graph. Values (mean  $\pm$  S.E.M.) are expressed as a percent of control (c) culture (100%) ( $n=5$ ). \* $P<0.05$  vs control. † $P<0.01$  vs control.

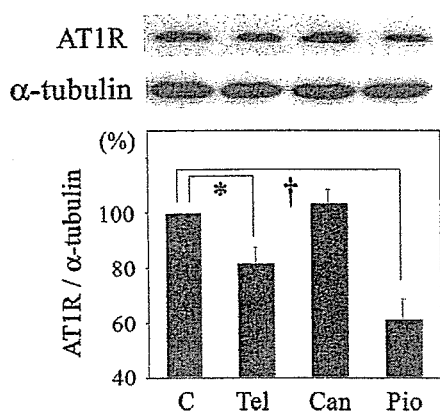


Fig. 3. Suppression of AT1R protein by telmisartan (Tel) but not by candesartan (Can) in VSMCs. VSMCs were incubated with Tel (10  $\mu$ mol/L, 12 h), Can (10  $\mu$ mol/L, 12 h), and Pio (10  $\mu$ mol/L, 6 h). Expression of AT1R protein and  $\alpha$ -tubulin was determined by Western blot analysis. Densitometric analysis was performed as described in the legend to Fig. 2. Values (mean  $\pm$  S.E. M.) are expressed as a percent of control (c) culture (100%) ( $n=5$ ). \* $P<0.05$  vs control. † $P<0.01$  vs control.

715 mmol/L 2-mercaptoethanol) at 95 °C for 3 min, electrophoresed on 12% SDS-polyacrylamide gel, and transferred to a polyvinylidene difluoride membrane (Immobilon-P, Millipore). The blots were blocked with TBS-T (20 mmol/L Tris-HCl [pH 7.6], 137 mmol/L NaCl, 0.1% Tween 20) containing 5% skim milk at room temperature for 30 min. The AT1R protein expressions were detected by ECL chemiluminescence (Amersham Pharmacia Biotech) according to the manufacturer's instructions. The membranes were exposed to X-ray film. The membranes were stripped by incubating them in a buffer containing 62.5 mmol/L Tris-HCl, 2% SDS, and 100 mmol/L 2-mercaptoethanol at 50 °C for 30 min and reprobed with an antibody against  $\alpha$ -tubulin by the same procedure. Phosphorylated ERK and ERK (which recognizes both phosphorylated and nonphosphorylated forms) were examined by the same method.

## 2.6. Statistical analysis

Statistical analysis was performed with 1- or 2-way ANOVA and Fisher test, if appropriate. Statistical significance was designated as  $P<0.05$ . Values are expressed as mean  $\pm$  S.E.M.

## 3. Results

### 3.1. Tel reduced the expression of AT1R

VSMCs were incubated with Tel (10  $\mu$ mol/L) for various periods. The expression level of AT1R mRNA was gradually decreased with a peak suppression at 6 h of incubation (Fig. 1). Though we did not remove Tel from the medium, the expression of AT1R demonstrated a transient suppression. The mechanism of its recovery at

12 h of incubation is unknown. However, there are some reports that demonstrated a transient or a biphasic gene expression induced by thiazolidinediones (TZDs) [23,24], which seems to be consistent with our results. Western blot analysis revealed that Tel reduced AT1R protein level with a peak reduction at 12 h of incubation (Fig. 2A), and that Tel suppressed AT1R expression in a dose-dependent manner (Fig. 2B). As shown in Fig. 2C, preincubation with Tel at the same concentration as used in Fig. 2B almost completely inhibited the Ang II-induced ERK phosphorylation.

Following experiment used 10  $\mu$ mol/L of Tel, which is the minimal dose that suppressed AT1R expression. Pio, one

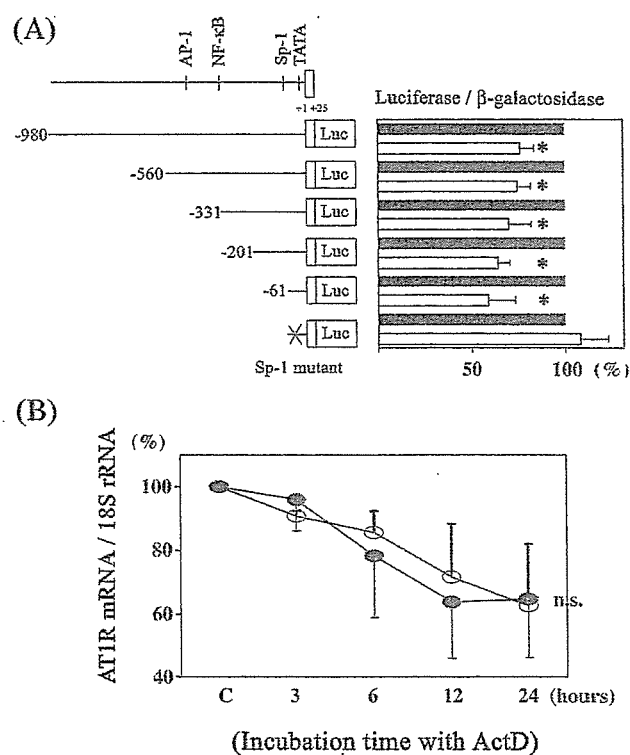


Fig. 4. Effect of telmisartan (Tel) on AT1R gene promoter activity and AT1R mRNA stability. (A) The scheme of deletion mutants of AT1R promoter/luciferase fusion DNA construct and SP-1 mutant construct is indicated. These luciferase constructs were introduced to VSMCs with LacZ expression plasmid by the DEAE-dextran method. Then VSMCs were stimulated with Tel (10  $\mu$ mol/L) for 12 h. Relative luciferase activity of unstimulated VSMCs (control) was set as 100%. Solid and open bars indicate the relative luciferase activity of unstimulated and Tel-stimulated VSMCs transfected with the same construct indicated in the left panel, respectively. Values (mean  $\pm$  S.E.M.) are expressed as a percent of control culture ( $n=6$ ). \* $P<0.05$  vs unstimulated cells. n.s. not significant. (B) VSMCs were incubated with Tel (10  $\mu$ mol/L) for 6 h and then ActD (5  $\mu$ g/mL) was added. In a control experiment, only ActD was added to the medium. Total RNA was isolated at the indicated time after ActD supplementation and expression levels of AT1R mRNA and rRNA were determined with method described in the legend to Fig. 1. Expression level of AT1R mRNA was normalized with that of rRNA. The normalized AT1R mRNA expression before addition of ActD in each group was set as 100% (c), ( $n=3$ ). n.s. not significant.

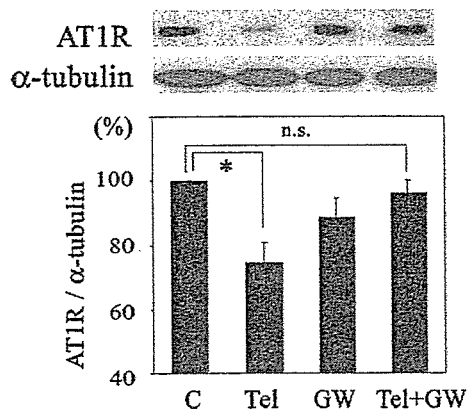


Fig. 5. The effect of GW9662, a PPAR  $\gamma$  antagonist, on telmisartan (Tel)-induced AT1R downregulation. VSMCs were preincubated with GW9662 (5  $\mu$ g/mL) for 30 min and incubated with or without Tel (10  $\mu$ mol/L) for 12 h. Expression of AT1R protein and  $\alpha$ -tubulin was determined by Western blot analysis. Densitometric analysis was performed as described in the legend to Fig. 2. Values (mean  $\pm$  S.E.M.) are expressed as a percent of control culture (100%) ( $n=5$ ). \* $P<0.05$  vs control. n.s. not significant.

of TZDs and a full PPAR $\gamma$  agonist, inhibited AT1R expression as previously described [16]. We examined the effect of other AT1R antagonists on AT1R expression. Can (Fig. 3) and Olm (data not shown) had no effect on AT1R expression.

### 3.2. Tel inhibits AT1R expression at the transcriptional level

Deletion mutants of AT1 promoter/luciferase fusion DNA were used to locate the response element responsible for Tel-induced AT1R suppression (Fig. 4A). The suppression was observed in all constructs from  $-980/+25$ -luc to  $-61/+25$ -luc, so we supposed that the response element may exist in the DNA segment between  $-61$  bp and  $+25$  bp. Since Sugawara et al. [16] had previously reported the crucial role of a GC-box-related sequence within the  $-58/-34$  region of the AT1R gene promoter in PPAR $\gamma$ -induced AT1R suppression, we hypothesized that the same site may also be important in Tel-induced suppression. The luciferase construct with mutation in GC box (Sp1 site) failed to respond to Tel (Fig. 4A), indicating the important role of Sp1 site in Tel-induced downregulation. In addition, Tel did not affect the degradation rate of AT1R mRNA (Fig. 4B). These data suggested that Tel inhibits AT1R gene transcription and does not affect AT1R mRNA stability.

### 3.3. Tel-induced AT1R downregulation is PPAR $\gamma$ dependent

To examine the role of PPAR $\gamma$  in Tel-induced AT1R suppression, we examined the effect of GW9662, a PPAR $\gamma$  antagonist. Although GW9662 itself did not affect AT1R expression, preincubation with GW9662 blocked AT1R suppression induced by Tel (Fig. 5).

## 4. Discussion

In the present study, we demonstrated that Tel, an AT1R antagonist, suppressed the AT1R expression through the PPAR $\gamma$ -mediated pathway. This is the first study that demonstrates the suppression of AT1R expression by AT1R antagonist in VSMCs.

The expression of AT1R was suppressed at both mRNA and protein levels. The results of the promoter assay and the mRNA stability assay suggested that the suppression occurred at the transcriptional level rather than the post-transcriptional level.

The involvement of PPAR $\gamma$  on AT1R suppression was confirmed by experiments using GW9662. GW9662 prevented the Tel-induced suppression of AT1R expression, indicating the critical role of PPAR $\gamma$  in this pathway. The ability to activate PPAR $\gamma$  is reported to be unique to Tel and irbesartan (Irb) among several AT1R antagonists [10]. In our study, though we have not examined the effect of Irb, Can (Fig. 3) and Olm (data not shown) had no effect on AT1R expression. Our results seem to be consistent with the previous report [10].

Schupp et al. reported that a subset of AT1R blockers (ARB), Tel and Irb, induced PPAR $\gamma$  activity and promoted PPAR $\gamma$ -dependent differentiation in 3T3-L1 adipocytes [9]. These ARB activated PPAR $\gamma$  by direct interaction with the ligand binding domain (LBD) of PPAR $\gamma$  [9].

The docking studies of the molecular binding model explained the difference in the ability to activate PPAR $\gamma$  among several ARB and full agonists of PPAR $\gamma$  by comparing their interaction with residues of several helices [10]. According to this model, Tel fits in the LBD of PPAR $\gamma$  surrounded by helices H3, H6, and H7. However, Tel does not interact with activation function-2 helix that is responsible for receptor activation and stabilization by full PPAR $\gamma$  agonists. Irb, Can, and Olm, so-called tetrazole-containing ARBs, made contact with helix H3 but not H7. The difference in the interaction with these helices of LBD of PPAR $\gamma$  might contribute to their potential to activate PPAR $\gamma$ .

On activation by a ligand, PPAR $\gamma$  regulates the expression of several genes involved in lipid and carbohydrate metabolism [25,26] and inflammatory responses [27]. From the molecular insight, these effects are basically due to two different transcriptional regulatory mechanisms, one is transactivation and the other is transrepression. Transactivation is dependent on PPAR $\gamma$  response element (PPRE). Upon activation, PPAR $\gamma$  forms a heterodimer with retinoid X receptor and binds to PPRE in the promoter region of the target genes such as CD36 and glucose transporter 4. In contrast, transrepression involves interference with other transcription factors such as NF- $\kappa$ B and AP-1. Because there is no consensus sequence of PPRE in the AT1R gene promoter up to  $-980$  bp, the suppression of AT1R gene transcription should have occurred through the latter mechanism.

This assumption is well substantiated by a previous study which reported that suppression of AT1R gene expression by



PPAR $\gamma$  activation was independent of PPRE [16]. The authors demonstrated that the –58/–34 region of the AT1R gene promoter, including Sp1 binding site, was essential to the PPAR $\gamma$  activator-induced AT1R suppression. They concluded that activated PPAR $\gamma$  inhibited Sp1 function by direct protein–protein interaction. Our study with Tel also demonstrated the essential role of Sp1 binding site in the suppression of AT1R expression. Therefore, Tel may inhibit Sp1 function through the activation of PPAR $\gamma$  resulting in downregulation of the AT1R expression.

Our previous studies showed that downregulation of AT1R by PPAR $\gamma$  activator attenuated cellular response to Ang II [15]. However, Ang II induced ERK activation was almost completely blocked by Tel even at 1  $\mu$ mol/L, which did not affect AT1R expression because of AT1R blocking effect (Fig. 2C). Therefore, AT1R binding effect is expected at the lower concentration of Tel and dual effect of AT1R binding and AT1R downregulation is expected at higher concentration.

TZDs, synthetic PPAR $\gamma$  activators, are reported to inhibit atherogenesis by regulating various gene expressions. Several studies have demonstrated the anti-atherogenic effects of PPAR $\gamma$  activators in both animal models and human. Rosiglitazone (Rosi), one of TZDs, was shown to have additive effects on plaque regression in the combination treatment with simvastatin in an atherosclerotic rabbit model [28]. Anti-atherogenic effect of Rosi was also reported in a diabetes–atherosclerosis mouse model [29]. AT1R antagonists are reported to suppress atherogenesis. Strawn et al. demonstrated that losartan attenuated atherogenesis in monkeys with hypercholesterolemia [30]. Based on these studies, Tel may be more efficient in suppressing atherosclerotic vascular diseases due to its properties of PPAR $\gamma$  activation and AT1R antagonism.

TZDs are also effective in improving insulin sensitivity and they are already utilized to treat patients with type 2 diabetes [31]. Although the precise mechanism for PPAR $\gamma$ -mediated insulin sensitization is not clear, TZDs reduced fasting and postprandial glucose concentration, and insulin level. Ang II also affects insulin sensitivity [32]. The inhibition of AT1R by losartan improved insulin sensitivity [33] and, in the LIFE study, losartan significantly reduced the incidence of new-onset diabetes in patients with hypertension compared with atenolol [34]. Therefore, the dual effects of Tel may synergistically improve insulin sensitivity.

The dual function of Tel, an AT1R antagonist and a partial agonist of PPAR $\gamma$ , may be quite useful for the treatment of patients with hypertension with complications such as diabetes and atherosclerosis. Considering the blockade of Ang II, the downregulation of AT1R through the activation of PPAR $\gamma$  adds further possibility of Tel. This may result in more complete inhibition of the Ang II. However, it remains to be determined whether Tel suppresses the expression of AT1R in vivo and is superior to other AT1R antagonists in terms of the inhibition of the progression of cardiovascular diseases. Further study is needed.

## Acknowledgements

This study was supported in part by grants from Takeda Science Foundation, Kimura Memorial Heart Foundation Research Grant for 2005, and Grants-in-aid for Scientific Research from the Ministry of Education, Culture, Sports, Science and Technology of Japan (17590742) to T.I.

## References

- [1] de Gasparo M, Catt KJ, Inagami T, Wright JW, Unger T. International union of pharmacology. XXIII. The angiotensin II receptors. *Pharmacol Rev* 2000;52:415–72.
- [2] Brenner BM, Cooper ME, de Zeeuw D, Keane WF, Mitch WE, Parving HH, et al. Effects of losartan on renal and cardiovascular outcomes in patients with type 2 diabetes and nephropathy. *N Engl J Med* 2001;345:861–9.
- [3] Diez J, Querejeta R, Lopez B, Gonzalez A, Larman M, Martinez Ubago JL. Losartan-dependent regression of myocardial fibrosis is associated with reduction of left ventricular chamber stiffness in hypertensive patients. *Circulation* 2002;105:2512–7.
- [4] Scheen AJ. Prevention of type 2 diabetes mellitus through inhibition of the renin–angiotensin system. *Drugs* 2004;64:2537–65.
- [5] Chiu AT, Herblin WF, McCall DE, Ardecky RJ, Carini DJ, Duncia JV, et al. Identification of angiotensin II receptor subtypes. *Biochem Biophys Res Commun* 1989;165:196–203.
- [6] Horiuchi M, Akishita M, Dzau VJ. Recent progress in angiotensin II type 2 receptor research in the cardiovascular system. *Hypertension* 1999;33:613–21.
- [7] Gillespie EL, White CM, Kardas M, Lindberg M, Coleman CI. The impact of ACE inhibitors or angiotensin II type 1 receptor blockers on the development of new-onset type 2 diabetes. *Diabetes Care* 2005;28:2261–6.
- [8] Healey JS, Baranchuk A, Crystal E, Morillo CA, Garfinkle M, Yusuf S, et al. Prevention of atrial fibrillation with angiotensin-converting enzyme inhibitors and angiotensin receptor blockers: a meta-analysis. *J Am Coll Cardiol* 2005;45:1832–9.
- [9] Schupp M, Janke J, Clasen R, Unger T, Kintscher U. Angiotensin type 1 receptor blockers induce peroxisome proliferator-activated receptor-gamma activity. *Circulation* 2004;109:2054–7.
- [10] Benson SC, Pershad Singh HA, Ho CI, Chittiboyina A, Desai P, Pravencu M, et al. Identification of telmisartan as a unique angiotensin II receptor antagonist with selective PPAR $\gamma$ -modulating activity. *Hypertension* 2004;43:993–1002.
- [11] Yki-Jarvinen H. Thiazolidinediones. *N Engl J Med* 2004;351:1106–18.
- [12] He W, Barak Y, Hevener A, Olson P, Liao D, Lc J, et al. Adipose-specific peroxisome proliferator-activated receptor gamma knockout causes insulin resistance in fat and liver but not in muscle. *Proc Natl Acad Sci U S A* 2003;100:15712–7.
- [13] Marx N, Kehrle B, Kohlhammer K, Grub M, Koenig W, Hombach V, et al. PPAR activators as anti-inflammatory mediators in human T lymphocytes: implications for atherosclerosis and transplantation-associated arteriosclerosis. *Circ Res* 2002;90:703–10.
- [14] Collins AR, Meehan WP, Kintscher U, Jackson S, Wakino S, Noh G, et al. Troglitazone inhibits formation of early atherosclerotic lesions in diabetic and nondiabetic low density lipoprotein receptor-deficient mice. *Arterioscler Thromb Vasc Biol* 2001;21:365–71.
- [15] Takeda K, Ichiki T, Tokunou T, Funakoshi Y, Iino N, Hirano K, et al. Peroxisome proliferator-activated receptor gamma activators downregulate angiotensin II type 1 receptor in vascular smooth muscle cells. *Circulation* 2000;102:1834–9.
- [16] Sugawara A, Takuchi K, Urano A, Ikeda Y, Arima S, Kudo M, et al. Transcriptional suppression of type 1 angiotensin II receptor gene expression by peroxisome proliferator-activated receptor-gamma in vascular smooth muscle cells. *Endocrinology* 2001;142:3125–34.

- [17] Yang H, Lu D, Raizada MK. Angiotensin II-induced phosphorylation of the AT1 receptor from rat brain neurons. *Hypertension* 1997;30:351–7.
- [18] Gupta M, Miller BA, Ahsan N, Ullsh PJ, Zhang MY, Cheung JY, et al. Expression of angiotensin II type I receptor on erythroid progenitors of patients with post transplant erythrocytosis. *Transplantation* 2000;70:1188–94.
- [19] Chomczynski P, Sacchi N. Single-step method of RNA isolation by acid guanidinium thiocyanate–phenol–chloroform extraction. *Anal Biochem* 1987;162:156–9.
- [20] Takeuchi K, Alexander RW, Nakamura Y, Tsujino T, Murphy TJ. Molecular structure and transcriptional function of the rat vascular AT1a angiotensin receptor gene. *Circ Res* 1993;73:612–21.
- [21] Guo DF, Uno S, Ishihata A, Nakamura N, Inagami T. Identification of a *cis*-acting glucocorticoid responsive element in the rat angiotensin II type 1A promoter. *Circ Res* 1995;77:249–57.
- [22] Sambrook J, Fritsch EF, Maniatis T. *Molecular cloning*. New York: Cold Spring Harbor Laboratory Press; 1989. p. 16.66–7.
- [23] Lin Y, Zhu X, McLntee FL, Xiao H, Zhang J, Fu M, et al. Interferon regulatory factor-1 mediates PPARgamma-induced apoptosis in vascular smooth muscle cells. *Arterioscler Thromb Vasc Biol* 2004;24:257–63.
- [24] Back SJ, Kim JS, Nixon JB, DiAugustine RP, Eling TE. Expression of NAG-1, a transforming growth factor-beta superfamily member, by troglitazone requires the early growth response gene EGR-1. *J Biol Chem* 2004;279:6883–92.
- [25] Tontonoz P, Hu E, Devine J, Beale EG, Spiegelman BM. PPAR gamma 2 regulates adipose expression of the phosphoenolpyruvate carboxykinase gene. *Mol Cell Biol* 1995;15:351–7.
- [26] Singh Ahuja H, Liu S, Crombie DL, Boehm M, Leibowitz MD, Heyman RA, et al. Differential effects of rexinoids and thiazolidinediones on metabolic gene expression in diabetic rodents. *Mol Pharmacol* 2001;59:765–73.
- [27] Diep QN, El Mabrouk M, Cohn JS, Endemann D, Amiri F, Viridis A, et al. Structure, endothelial function, cell growth, and inflammation in blood vessels of angiotensin II-infused rats: role of peroxisome proliferator-activated receptor-gamma. *Circulation* 2002;105:2296–302.
- [28] Tao L, Liu HR, Gao E, Teng ZP, Lopez BL, Christopher TA, et al. Antioxidative, antinflammatory, and vasculoprotective effects of a peroxisome proliferator-activated receptor-gamma agonist in hypercholesterolemia. *Circulation* 2003;108:2805–11.
- [29] Phillips JW, Barringhaus KG, Sanders JM, OYang Z, Chen M, Hesselbacher S. Rosiglitazone reduces the accelerated neointima formation after arterial injury in a mouse injury model of type 2 diabetes. *Circulation* 2003;108:1994–9.
- [30] Strawn WB, Chappell MC, Dean RH, Kivlighn S, Ferrario CM. Inhibition of early atherogenesis by losartan in monkeys with diet-induced hypercholesterolemia. *Circulation* 2000;101:1586–93.
- [31] Miyazaki Y, Mahankali A, Matsuda M, Glass L, Mahankali S, Ferrannini E. Improved glycemic control and enhanced insulin sensitivity in type 2 diabetic subjects treated with pioglitazone. *Diabetes Care* 2001;24:710–9.
- [32] Velloso LA, Folli F, Sun XJ, White MF, Saad MJ, Kahn CR. Cross-talk between the insulin and angiotensin signaling systems. *Proc Natl Acad Sci U S A* 1996;93:12490–5.
- [33] Olsen MH, Fossum E, Hoiieggen A, Wachtell K, Hjerkin E, Nesbitt SD. Long-term treatment with losartan versus atenolol improves insulin sensitivity in hypertension: ICARUS, a LIFE substudy. *J Hypertens* 2005;23:891–8.
- [34] Lindholm LH, Ibsen H, Borch-Johnsen K, Olsen MH, Wachtell K, Dahlöf B. Risk of new-onset diabetes in the losartan intervention for endpoint reduction in hypertension study. *J Hypertens* 2002;20:1879–86.

## A third-generation, long-acting, dihydropyridine calcium antagonist, azelnidipine, attenuates stent-associated neointimal formation in non-human primates

Kaku Nakano<sup>a</sup>, Kensuke Egashira<sup>a</sup>, Hideo Tada<sup>a</sup>, Yoshiro Kohjimoto<sup>b</sup>, Yasuhiko Hirouchi<sup>b</sup>, Shun-ichi Kitajima<sup>b</sup>, Yasuhisa Endo<sup>c</sup>, Xiao-Hang Li<sup>d</sup> and Kenji Sunagawa<sup>a</sup>

**Background** Calcium antagonists have been shown to reduce atherogenesis and improve clinical outcomes in atherosclerotic vascular disease. No study has so far, however, addressed the effects of calcium antagonists on stent-associated neointimal formation. We therefore investigated whether a third-generation calcium antagonist, azelnidipine, attenuates in-stent neointimal formation in non-human primates.

**Method** Male cynomolgus monkeys were fed a high cholesterol diet for 4 weeks, and were randomly assigned to three groups: a vehicle group and two other groups treated with azelnidipine at 3 and 10 mg/kg per day for an additional 24 weeks ( $n = 12$  each). Multi-link stents were then implanted in the iliac artery.

**Results** Azelnidipine at the high dose reduced neointimal thickness ( $0.25 \pm 0.02$  versus  $0.19 \pm 0.02$  mm;  $P < 0.05$ ). Azelnidipine also reduced local oxidative stress and monocyte chemoattractant protein 1 (MCP-1) expression. No difference was found between the three groups in the degrees of injury score, inflammation score, plaque neovascularization, or plasma lipid levels. Azelnidipine also reduced MCP-1-induced proliferation/migration of vascular smooth muscle cells *in vitro*.

**Conclusions** This study demonstrated for the first time that azelnidipine attenuates in-stent neointimal

formation associated with the reduced expression of MCP-1 and smooth muscle proliferation/migration in the neointima. These data in non-human primates suggest potential clinical benefits of azelnidipine as a 'vasculoprotective calcium antagonist' in patients undergoing vascular interventions. *J Hypertens* 24:1881–1889 © 2006 Lippincott Williams & Wilkins.

Journal of Hypertension 2006, 24:1881–1889

Keywords: monocyte, neointimal hyperplasia, restenosis, smooth muscle cell

<sup>a</sup>Department of Cardiovascular Medicine, Graduate School of Medical Sciences, Kyushu University, Fukuoka, Japan, <sup>b</sup>Primate Research Center, Guandong, China, <sup>c</sup>Department of Applied Biology, Kyoto Institute of Technology, Kyoto, Japan and <sup>d</sup>Gaoyao Kangda Laboratory Animal Science and Technology, Guandong, China

Correspondence and requests for reprints to Kensuke Egashira, MD, PhD, Department of Cardiovascular Medicine, Graduate School of Medical Science, Kyushu University, 3-1-1 Maidashi, Higashi-ku, Fukuoka 812-8582, Japan Tel: +81 92 642 5358; fax: +81 92 642 5375; e-mail: egashira@cardiol.med.kyushu-u.ac.jp

Sponsorship: This study was supported by grants-in-aid for scientific research (nos. 14657172 and 14207036) from the Ministry of Education, Science, and Culture, Tokyo, Japan, by health science research grants (Comprehensive Research on Aging and Health, and Research on Translational Research) from the Ministry of Health Labor and Welfare, Tokyo, Japan, and by the Program for the Promotion of Fundamental Studies in Health Sciences of the Organization for Pharmaceutical Safety and Research, Tokyo, Japan.

Received 19 September 2005 Revised 10 April 2006 Accepted 12 April 2006

### Introduction

Dihydropyridine calcium antagonists have been used worldwide for patients with hypertension and atherosclerotic vascular disease. Recent clinical trials with calcium antagonists provided evidence suggesting that reducing arterial blood pressure close to normal ranges is of great importance in reducing cardiovascular events [1–4]. Notably, in the Comparison of Amlodipine versus Enalapril to Limit Occurrences of Thrombosis (CAMELOT) trial [5], compared with placebo and enalapril, the third-generation calcium antagonist amlodipine was shown to reduce hospitalization as a result of unstable angina and revascularization in patients with coronary artery disease already being treated with aspirin, beta-blockers, or statins. These latest clinical trials suggest that there might be pleiotropic actions of cal-

cium antagonists beyond blood pressure lowering. The pleiotropic actions of calcium antagonists may be distinct from pharmacological actions related to L-type calcium channel blockade, but may be attributable to their lipophilic character leading to a high affinity with membrane phospholipid of arterial wall cells such as vascular smooth muscle cells (VSMC) [6]. The vasculoprotective actions of such calcium antagonists include an improvement in endothelial function, an anti-inflammation effect, anti-oxidant function, antiproliferation of VSMC and so forth.

In animal experiments, calcium antagonists have been shown to prevent or attenuate atherosclerosis [7,8], hypertension-induced vascular remodeling [9], heart failure [10] and neointimal formation after balloon injury [11]. However, no study has so far addressed the effects of

calcium antagonists on stent-associated neointimal formation. Investigating this subject must be of clinical importance, because stent implantation is now the major revascularization technique worldwide in patients with atherosclerotic vascular disease. Although a drug-eluting stent reduces the restenosis rate in selected arterial lesions, stent-associated restenosis remains an unsolved clinical issue in high-risk lesions. The cellular mechanism of restenosis after stenting is presumed to be neointimal formation as a result of VSMC proliferation/migration, recruitment of bone marrow-derived progenitor cells or inflammation in response to injury [12–14].

Azelnidipine is a newly developed third-generation calcium antagonist and has antihypertensive action that is comparable to amlodipine [15]. Azelnidipine has strong lipophilicity and affinity to membranes of VSMC [16,17]. Therefore, the aim of this study was to investigate whether azelnidipine at a clinical dose range attenuates in-stent neointimal formation in non-human primates (cynomolgus monkeys). To gain clinical significance for the results obtained, we used a non-human primate model of stent-associated neointimal formation [12].

## Materials and methods

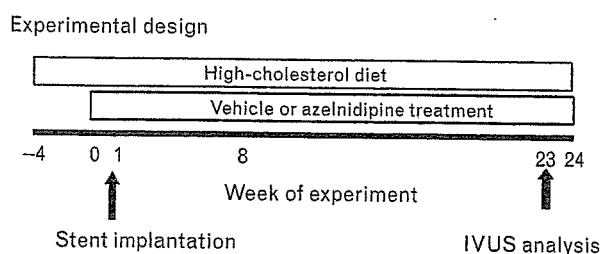
### Experimental animals

Thirty-six 5-year-old male cynomolgus monkeys weighing 4.2–6.6 kg were purchased. The study protocol was reviewed and approved by the Committee on the Ethics of Animal Experiments, Kyushu University Graduate School of Medical Sciences. The animal care before and after the operation of the animal model was performed in Gaoyao Kangda Laboratory Animal Science and Technology in China. A part of this study was performed at the Station for Collaborative Research and the Morphology Core, Kyushu University Graduate School of Medical Sciences.

### Animal model of in-stent restenosis

All animals were fed a high-cholesterol diet (0.5% cholesterol and 6% corn oil) for 4 weeks before stent implantation (Fig. 1). Ticlopidine 100 mg and aspirin 81 mg were started 7 days before the initial procedure. Aspirin was to be given and continued until animals were killed at

Fig. 1



Experimental design. IVUS, Intravascular ultrasound.

6 months, and ticlopidine was administered for 28 days. The animals were randomly assigned to three groups as follows: (i) no treatment vehicle control group (0.5% carboxymethyl cellulose sodium salt); (ii) low-dose azelnidipine (3 mg/kg per day; donated by Sankyo Pharmaceutical Co., Tokyo, Japan) group; (iii) high-dose azelnidipine (10 mg/kg per day) group ( $n = 12$  each). Azelnidipine treatment was carried out once a day by gavage for 24 weeks. One week after grouping, all monkeys were anaesthetized with ketamine hydrochloride (10 mg/kg intramuscularly) and sodium pentobarbital (30 mg/kg intravenously), and underwent the placement of a 15 mm-long Multilink stent mounted over the 3-mm balloon implanted in the iliac artery (30 s inflation at 6 atm followed by 60 s inflation at 8 atm, resulting in a stent-to-artery ratio of 1.2 : 1.0) as described [12]. After the operation, all monkeys were fed the same high-cholesterol diet.

### Histopathology and immunohistochemistry

Stented arterial sections were excised and fixed for 24 h with 95% ethanol and 1% acetic acid. Each segment was divided into two parts at the centre of the stent. The proximal part was embedded in methyl methacrylate mixed with *n*-butyl methacrylate to allow for sectioning through metal stent struts. Serial sections were stained with elastica van Gieson and haematoxylin eosin. To evaluate the stent area, lumen area, medial area, and neointimal area, the neointimal thickening (neointimal area/length of internal elastica lamina; IEL) were measured. An immunohistochemical study was performed with antibodies against human smooth muscle actin (1A4; Dako, Tokyo, Japan) and von Willebrand factor (vWF; Dako). To evaluate the degree of neo-vascularization the number of arterioles in the intima and adventitia were counted.

The distal part was used for immunohistochemical analysis. After stent struts were gently removed with micro forceps, the tissue was dehydrated, embedded in paraffin, and cut into 5- $\mu$ m thick slices. They were subjected to immunostaining using antibodies against human monocyte chemoattractant protein 1 (MCP-1; Santa Cruz, California, USA) and C-C chemokine receptor 2 (CCR2, Santa Cruz) as described [12]. A single observer, who was blinded to the experiment protocol, performed the morphometry. All images were captured by an Olympus microscope equipped with a digital camera (HC-2500) and were analysed using Adobe Photoshop 6.0 (Adobe Systems, San Jose, California, USA) and Scion Image 1.62 (Scion, Frederick, Maryland, USA) software.

### Local oxidative stress with fluorescent dihydroethidium micrographic analysis

Frozen, enzymatically intact, sections (10- $\mu$ m thick) just at the proximal edge of stented iliac arteries were incubated with dihydroethidium (10  $\mu$ mol/l; Sigma, Tokyo,